ASSESSMENT OF MECHANICAL RESPONSE OF DRIP SHIELDS UNDER REPOSITORY ENVIRONMENT—PROGRESS REPORT 2

Prepared for

U.S. Nuclear Regulatory Commission
Contract NRC–02–97–009

Prepared by

G. Douglas Gute
Amitava Ghosh
Sui-Min Hsiung
Asadul H. Chowdhury

Center for Nuclear Waste Regulatory Analyses
San Antonio, Texas

November 2001

EXECUTIVE SUMMARY

Rockfall onto components of the engineered barrier subsystem is a potential disruptive event that needs to be considered when evaluating the performance characteristics of the proposed geologic repository for spent nuclear fuel and high-level waste at Yucca Mountain, Nevada. Rockfall can conceivably damage the drip shield and waste package components of the engineered barrier subsystem, thereby degrading their ability to perform their intended functions. Falling rock blocks impacting the drip shield may open infiltration pathways that would allow water to contact the waste package, both enabling and accelerating various corrosion processes that may reduce the service life of the waste package. Moreover, sufficiently large rock blocks could rupture the waste package outright, creating open pathways for water entry and radionuclide release into the emplacement drifts. The U.S. Nuclear Regulatory Commission (NRC) and the Center for Nuclear Waste Regulatory Analyses are developing an abstracted model to assess the potential effects of rockfall. This model will be used in evaluating the proposed geologic repository design. This abstraction will be capable of (i) checking and verifying U.S. Department of Energy (DOE) design calculations, (ii) identifying important contributing factors that must be considered, and (iii) being incorporated into the NRC Total-system Performance Assessment code so that the influence of rockfall on off-site dose for the 10,000-year regulatory period can be accounted.

The objective of the work presented in this report is the improvement of the current rockfall abstraction model presently employed within the SEISMO module of the NRC Total-system Performance Assessment code. The Total-system Performance Assessment code will be used to probe and independently evaluate the DOE demonstration of compliance with NRC regulations.

Specific issues addressed in this report are the effects of rock block size and shape, engineered barrier subsystem component temperatures, and seismic ground motion on the ability of the drip shield to mitigate damage to the waste package by rockfall. From a finite element modeling perspective, the report provides information pertaining to the (i) individual element type used, (ii) mesh density, (iii) capabilities and limitations of the code itself, (iv) various boundary conditions implemented within the model, and (v) rock block and drip shield material constitutive models. Preliminary results obtained from a parametric study presently being performed are presented as well. The parametric study has been designed to identify the significant variables of the rockfall problem and subsequently assess their influence on the various engineered barrier subsystem components.

Previous studies indicated that a finely refined mesh in the region of the rock block that defines the contact interface with the drip shield can predict the onset of crushing, fracturing, and splintering of the rock. Simply assuming that the rock block will behave in a purely linear elastic manner, however, will typically lead to conservative estimates of the drip shield stresses and deformations. Therefore, the development of an appropriate rock failure criterion that could be used to remove individual elements from the rock block model before they become numerically unstable and cause the analysis to terminate prematurely has been deferred indefinitely.

The drip shield and rock block impact simulation also indicates that ground motion effects may play an important role in the magnitude of the forces that the impacted engineered barrier subsystem components will experience. To understand these effects, potential resonance of

the individual engineered barrier subsystem component structures generated by the seismic ground motion and development of concomitant dynamic load amplification factors should continue to be studied. These effects are strongly dependent on the design details of the engineered barrier subsystem components and the time–history characterization that defines the seismic ground motion for the proposed Yucca Mountain repository horizon.

The drip shield and rock block impact analyses were performed for three different cases: 0.5-, 1.0-, and 2.0-tonne (1,102-, 2,205-, and 4,409-lb) rock blocks per drip shield segment length. The drip shield deflections can be quite large, even for these relatively small rock blocks. The clearances between the drip shield and different waste package types vary in the range 0.080–0.592 m (0.262–0.194 ft). It was determined that rock blocks characterized as greater than 1.0-tonne (2,205-lb) per drip shield segment length are sufficient to drive the drip shield into the defense high-level waste package. Specifically, the 1.0-tonne (2,205-lb) rock block per drip shield segment length will deform the drip shield 0.097 m (0.318 ft), and a 2.0-tonne (4,409-lb) rock block per drip shield segment length will deform the drip shield 0.174 m (0.571 ft).

Additional results obtained from the finite element analyses of the drip shield and rock block impact problem are the level of stresses experienced by the different drip shield components, (i.e., the titanium grade 7 plates and titanium grade 24 bulkhead and support beam structural stiffeners during the impact event). The Von Mises stress does not exceed the titanium grade 24 yield stress of 658.1 MPa (95.5 ksi) in the bulkhead or support beam for the 0.5-tonne (1,102-lb) per drip shield segment length impact load. The 1.0- and 2.0-tonne (2,205- and 4,409-lb) rock block impact per drip shield segment length loads, on the other hand, indicate that the bulkhead stress level has exceeded the titanium grade 24 yield stress. In the case of the 2.0-tonne (4,409-lb) per drip shield segment length impact load, the support beam has also experienced Von Mises stresses beyond the titanium grade 24 yield stress.

The yield stress for titanium grade 7, 174.1 Mpa, (25.3 ksi), is significantly smaller than the 658.1 MPa (95.5 ksi) yield stress for titanium grade 24. It was found that, even for the 0.5-tonne (1,102 lb) rock block case, the titanium grade 7 yield stress was exceeded in the drip shield plates. It needs to be emphasized that the drip shield plate has been modeled with a 2-cm (0.787-in.) thickness, not the 1.5-cm (0.591-in.) thickness defined in recent DOE documents. As a result, the stress levels in the drip shield plate were underestimated in the analyses.

Drip shield components subjected to Von Mises stress magnitudes greater than their material's yield stress have incurred some plastic deformation and may be susceptible to stress corrosion cracking because of the residual stresses remaining after the impact event.

None of the cases evaluated resulted in Von Mises stress magnitudes that exceeded the ultimate tensile strengths of titanium grade 7 or titanium grade 24, which would be indicative of the drip shield being breached. It needs to be emphasized, however, that the sizes of the impacting rock blocks evaluated thus far are considered to be relatively small.

4/55

CONTENTS

Section Page

EXECUTIVE SUMMARY iii
FIGURES vii
TABLES ix
ACKNOWLEDGMENTS xi

1 INTRODUCTION 1-1
1.1 BACKGROUND 1-1
1.2 OBJECTIVE AND SCOPE 1-2

2 FINITE ELEMENT ROCK BLOCK AND DRIP SHIELD IMPACT MODELING STUDY .. 2-1
2.1 FINITE ELEMENT MODELING OF THE DRIP SHIELD 2-1
2.1.1 Drip Shield Model 2-1
2.1.2 Drip Shield Material Constitutive Models 2-3
2.2 FINITE ELEMENT MODELING OF THE ROCK BLOCK 2-7
2.3 DRIP SHIELD AND ROCK BLOCK IMPACT CONDITIONS 2-8
2.3.1 Modeling Seismic Ground Motion Effects 2-9
2.3.2 Modeling the Drip Shield Contact Interactions 2-10

3 DRIP SHIELD AND ROCK BLOCK IMPACT ANALYSIS RESULTS 3-1

4 SUMMARY OF ANALYSIS RESULTS AND FUTURE PLAN 4-1
4.1 SUMMARY OF RESULTS 4-1
4.2 FUTURE PLAN 4-1

5 REFERENCES 5-1

APPENDIX

5/55

FIGURES

Figure		Page
1-1	Illustration of the Drip Shield Design Proposed by the U.S. Department of Energy . .	1-4
2-1	Schematic of the Proposed Engineered Barrier Subsystem	2-11
2-2	Schematic Illustrating the Symmetry Planes Used to Simplify the Finite Element Model.	2-12
2-3a	Drip Shield–Rock Block Impact Finite Element Model	2-13
2-3b	Drip Shield–Rock Block Impact Finite Element Model	2-14
2-4	Schematic of the Engineering Stress-Engineering Strain Curve for Titanium Grade 7 at 150 °C (302 °F)	2-15
2-5	Schematic of the Engineering Stress-Engineering Strain Curve for Titanium Grades 5 and 24 at 150 °C (302 °F)	2-16
2-6	Schematic of the True Stress-Logarithmic Strain Curve for Titanium Grade 7 at 150 °C (302 °F)	2-17
2-7	Schematic of the True Stress-Logarithmic Strain Curve for Titanium Grades 5 and 24 at 150 °C (302 °F)	2-18
2-8	Schematic of the Engineering Stress-Engineering Strain Curve for Alloy 22 at 150 °C (302 °F)	2-19
2-9	Schematic of the True Stress-Logarithmic Strain Curve for Alloy 22 at 150 °C (302 °F)	2-20
3-1	Drip Shield Deflections for Various Rock Block Impact Cases	3-4
3-2	Von Mises Stress (MPa) Distribution in the Drip Shield at the Maximum Deflection Point due to a 0.5-tonne (1,102-lb) Rock Block Impact per Drip Shield Segment Length	3-5
3-3	Von Mises Stress (MPa) Distribution in the Drip Shield at the Maximum Deflection Point due to a 1.0-tonne (2,205-lb) Rock Block Impact per Drip Shield Segment Length	3-6
3-4	Von Mises Stress (MPa) Distribution in the Drip Shield at the Maximum Deflection Point due to a 2.0-tonne (4,409-lb) Rock Block Impact per Drip Shield Segment Length	3-7
3-5	Von Mises Stress (MPa) Distribution in the 2-cm (0.787-in.) Thick Titanium Grade 7 Drip Shield Plate at the Maximum Deflection Point due to a 0.5-tonne (1,102-lb) Rock Block Impact	3-8
3-6	Von Mises Stress (MPa) Distribution in the 2-cm (0.787 in.) Thick Titanium Grade 7 Drip Shield Plate at the Maximum Deflection Point due to a 1.0-tonne (2,205-lb) Rock Block Impact	3-9
3-7	Von Mises Stress (MPa) Distribution in the 2-cm (0.787 in.) Thick Titanium Grade 7 Drip Shield Plate at the Maximum Deflection Point due to a 2.0-tonne (4,409-lb) Rock Block Impact	3-10
3-8	Maximum Von Mises Stress (MPa) Level Incurred by the Drip Shield Bulkhead due to a 0.5-tonne (1,102-lb) Rock Block Impact per Drip Shield Segment Length	3-11
3-9	Maximum Von Mises Stress (MPa) Level Incurred by the Drip Shield Support Beam due to a 0.5-tonne (1,102-lb) Rock Block Impact per Drip Shield Segment Length .	3-12
3-10	Maximum Von Mises Stress (MPa) Level Incurred by the 2-cm (0.787-in.) Thick Drip	

3-10 Maximum Von Mises Stress (MPa) Level Incurred by the 2-cm (0.787-in.) Thick Drip Shield Plate due to a 0.5-tonne (1,102-lb) Rock Block Impact per Drip Shield Segment Length 3-13
3-11 Maximum Von Mises Stress (MPa) Level Incurred by the Drip Shield Bulkhead due to a 1.0-tonne (2,205-lb) Rock Block Impact per Drip Shield Segment Length 3-14
3-12 Maximum Von Mises Stress (MPa) Level Incurred by the Drip Shield Support Beam due to a 1.0-tonne (2,205-lb) Rock Block Impact per Drip Shield Segment Length . 3-15
3-13 Maximum Von Mises Stress (MPa) Level Incurred by the 2-cm (0.787-in.) Thick Drip Shield Plate due to a 1.0-tonne (2,205-lb) Rock Block Impact per Drip Shield Segment Length 3-16
3-14 Maximum Von Mises Stress (MPa) Level Incurred by the Drip Shield Bulkhead due to a 2.0-tonne (4,409-lb) Rock Block Impact per Drip Shield Segment Length 3-17
3-15 Maximum Von Mises Stress (MPa) Level Incurred by the Drip Shield Support Beam due to a 2.0-tonne (4,409-lb) Rock Block Impact per Drip Shield Segment Length . 3-18
3-16 Maximum Von Mises Stress (MPa) Level Incurred by the 2-cm (0.787-in.) Thick Drip Shield Plate due to a 2.0-tonne (4,409-lb) Rock Block Impact per Drip Shield Segment Length 3-19

7/55

TABLES

Table		Page
2-1	Relevant Mechanical Properties of Titanium Grade 7 as a Function of Temperature According to the 1995 American Society of Mechanical Engineers Boiler & Pressure Vessel Code	2-4
2-2	Relevant Mechanical Properties of Titanium Grade 7 as a Function of Temperature According to the 1998 American Society of Mechanical Engineers Boiler & Pressure Vessel Code	2-5
2-3	Relevant Mechanical Properties of Titanium Grade 5 as a Function of Temperature	2-5
2-4	Relevant Mechanical Properties of Alloy 22 as a Function of Temperature According to the 1998 American Society of Mechanical Engineers Boiler & Pressure Vessel Code	2-6
2-5	Elastic Material Properties Used for the Rock Block Mass	2-8
3-1	Clearances Between the Drip Shield and Different Waste Package Types	3-1

8/55

ACKNOWLEDGMENTS

This report was prepared to document work performed by the Center for Nuclear Waste Regulatory Analyses (CNWRA) for the U.S. Nuclear Regulatory Commission (NRC) under Contract No. NRC–02–97–009. The activities reported here were performed on behalf of the NRC Office of Nuclear Material Safety and Safeguards, Division of Waste Management. The report is an independent product of the CNWRA and does not necessarily reflect the views or regulatory position of the NRC.

The authors thank S. Mayer and B. Sagar for their reviews of this report. The authors are thankful to C. Patton for assisting with the word processing and preparation of the final report and to B. Long and C. Cudd for editorial reviews.

QUALITY OF DATA, ANALYSES, AND CODE DEVELOPMENT

DATA: All CNWRA-generated original data contained in this report meet quality assurance requirements described in the CNWRA Quality Assurance Manual. Sources for other data should be consulted for determining the level of quality for those data.

ANALYSES AND CODES: Finite element analyses in this report were conducted by the CNWRA using the commercial computer code ABAQUS/Explicit Version 5.8-16. Pre- and post-processing of the finite element models were accomplished using the commercial computer code HyperMesh. ABAQUS/Explicit and HyperMesh are controlled under the CNWRA software quality assurance procedure (TOP-018, Development and Control of Scientific and Engineering Software). Spreadsheet calculations were accomplished using Microsoft Excel 97 SR–2. Details of the finite element modeling simplifications and procedures used to generate the results presented in this report can be found in CNWRA scientific notebook number 391.

9/55

1 INTRODUCTION

1.1 BACKGROUND

The U.S. Department of Energy (DOE) has been studying the Yucca Mountain site in Nevada for more than 15 years to determine whether it is a suitable site for building a geologic repository for the nation's spent nuclear fuel and high-level waste (CRWMS M&O, 2001). The proposed repository design employs an engineered barrier subsystem in concert with the desert environment and geologic features of Yucca Mountain for the purpose of keeping water away from the spent nuclear fuel and high-level waste for thousands of years. Two primary components of the engineered barrier subsystem are the drip shield and waste package (CRWMS M&O, 2001). Other potential components of the engineered barrier subsystem include backfill and emplacement drift seals. The basic concept of the proposed geologic disposal at Yucca Mountain is the placement of carefully prepared and packaged nuclear waste in excavated tunnels in tuff about 350 m (1,148 ft) below the surface and 225 m (738 ft) above the water table. In this condition, the engineered barriers are intended to work with the natural barriers—the geology and climate of Yucca Mountain—to contain and isolate the nuclear waste for thousands of years. For example, the evolving engineered barrier component designs include materials chosen to be compatible with the underground thermal and geochemical environment, and the layout of tunnels takes into consideration the geology of the mountain (CRWMS M&O, 2001).

Through successive evaluations, the repository design evolved to the Viability Assessment reference design (DOE, 1998a,b). This reference design represented a snapshot of the ongoing design process, thus providing a frame of reference to describe how the proposed repository at Yucca Mountain could function. Following presentation of the Viability Assessment reference design for the proposed repository to the U.S. Congress, the License Application Design Selection project was completed by DOE (CRWMS M&O, 1999a,b,c). The goal of the License Application Design Selection project was to develop and evaluate a diverse range of conceptual repository designs that would be compatible with the geologic attributes of the Yucca Mountain site and to recommend an initial design concept for the possible Site Recommendation and License Application documents. Ultimately, the potential benefits of five variations of the Viability Assessment reference design were studied to identify design attributes that could improve the functional characteristics of the proposed repository. A new repository reference design has been adopted as a result of this exercise. This new design, referred to as Enhanced Design Alternative II, uses more extensive thermal management techniques than the Viability Assessment design to redirect water flow through the rock mass between the emplacement drifts (CRWMS M&O, 1999b). The new Enhanced Design Alternative II also differs from the Viability Assessment design in that steel structural materials are now primarily used in the drifts instead of concrete to avoid possible adverse chemical reactions pertaining to corrosion, as well as mobilization and movement of radionuclides.

Even though the repository design strategy was brought further into focus by the Yucca Mountain Science and Engineering Report (CRWMS M&O, 2001), the design details for the individual engineered barrier subsystem components continue to evolve. Although the primary objective of the drip shield is to divert water from the waste package, the DOE is taking credit for the drip shield dissipating a significant portion of the kinetic energy associated with rockfall

and, as a result, limiting the potential number of waste packages that may be breached because of this form of mechanical disruption (CRWMS M&O, 2001).

From the perspective of mechanical disruption of the engineered barrier subsystem, the U.S. Nuclear Regulatory Commission (NRC) and the Center for Nuclear Waste Regulatory Analyses (CNWRA) focused their efforts on identifying the critical variables that directly influence waste package performance as they relate to seismicity, faulting, rockfall, and igneous activity without accounting for the mitigating effects of other engineered barrier components as evidenced by Mohanty, et al. (2000), Ghosh, et al. (1998), Hill and Trapp (1997), and Gute, et al. (1999). Ongoing and future NRC activities on the effects of faulting and volcanism on waste package performance have been discussed in the appropriate NRC issue resolution status reports (NRC, 2000a,b; CNWRA, 2001; Hill and Connor, 2000).

With regard to seismicity and rockfall, the DOE conducted a drift degradation analysis study (CRWMS M&O, 1999d, 2000a) that uses Yucca Mountain site data to assess the potential size and number of key blocks along the length of the emplacement drifts for varying drift orientations. The study used a quasi-static approach to analyze the effects of seismic ground motion on key block characterization for a fixed drift orientation of 105 degrees. There are several aspects of this report that warrant closer scrutiny by the NRC and CNWRA because its findings will provide part of the design basis parameters pertaining to seismically induced rockfall for the engineered barrier subsystem components. As part of its independent assessment of key parameters affecting repository performance, potential rockfall block sizes and areal coverage of rockfall in the emplacement drifts arising from seismicity are being investigated in a separate study by the CNWRA (Hsiung, et al., 2000, 2001).

1.2 OBJECTIVE AND SCOPE

The current SEISMO module that evaluates the potential for direct rupture of waste packages from rockfall induced by seismicity is based on many simplifying assumptions. It is not clear at this time whether the presumably conservative failure criterion used within the current SEISMO module is sufficient to account for these effects on waste package integrity (Gute, et al., 1999). The objective of this study is to improve the rockfall abstraction presently employed within the SEISMO module of the NRC Total-system Performance Assessment code by ensuring that all the critical variables have been identified and that all design features are accounted for. The activities ongoing to meet this objective include

- Develop finite element analysis models capable of simulating the rock block and waste package impact event caused by seismically induced rockfall. These models will be used to determine the relative significance of the following parameters:
  - Rock block size and shape
  - Relative velocity between the falling rock block and waste package during the seismic event
  - Long-term corrosion-related degradation of the waste package
  - Initial manufacturing defects
  - Residual stresses and potential loss of material ductility in the immediate area of the waste package closure weld
  - Material embrittlement

11/55

  - Temperature effects
  - Seismic shaking of the waste packages

- Establish relationships between the extent of the localized damage to the waste packages and the effects enumerated in the previous bullet

- Develop a realistic failure criterion for predicting waste package ruptures

Although it is not certain that the drip shield will remain part of the DOE engineered barrier subsystem design strategy given its high cost, the reliance DOE places on the ability of the drip shield to protect the waste package from rockfall reinforces the need for staff to account for the mitigating effects of the drip shield in the SEISMO module (Mohanty et al., 2000). This report focuses on assessing the performance characteristics of the most recent drip shield design proposed to be used by DOE (CRWMS M&O, 2000b, 2001) as shown in Figure 1-1. Specifically, this report conveys the preliminary results obtained from a parametric study being performed to approximate and assess the effects of rock block size and fall height, engineered barrier subsystem component temperatures, and seismic ground motion on the ability of the drip shield to mitigate damage to the waste package by rockfall. The SEISMO module abstraction will be updated by integrating the results of the drip shield parametric study with the waste package failure criterion work. In addition, the analytical results obtained from this effort can provide engineering insight to the relative significance of the aforementioned factors (i.e., temperature effects, corrosion-induced long-term degradation of the waste package, and such). The analyses presented in this report were conducted with the finite element code ABAQUS/Explicit Version 5.8-16 (Hibbitt, Karlsson & Sorenson, Inc., 1998).

12/55

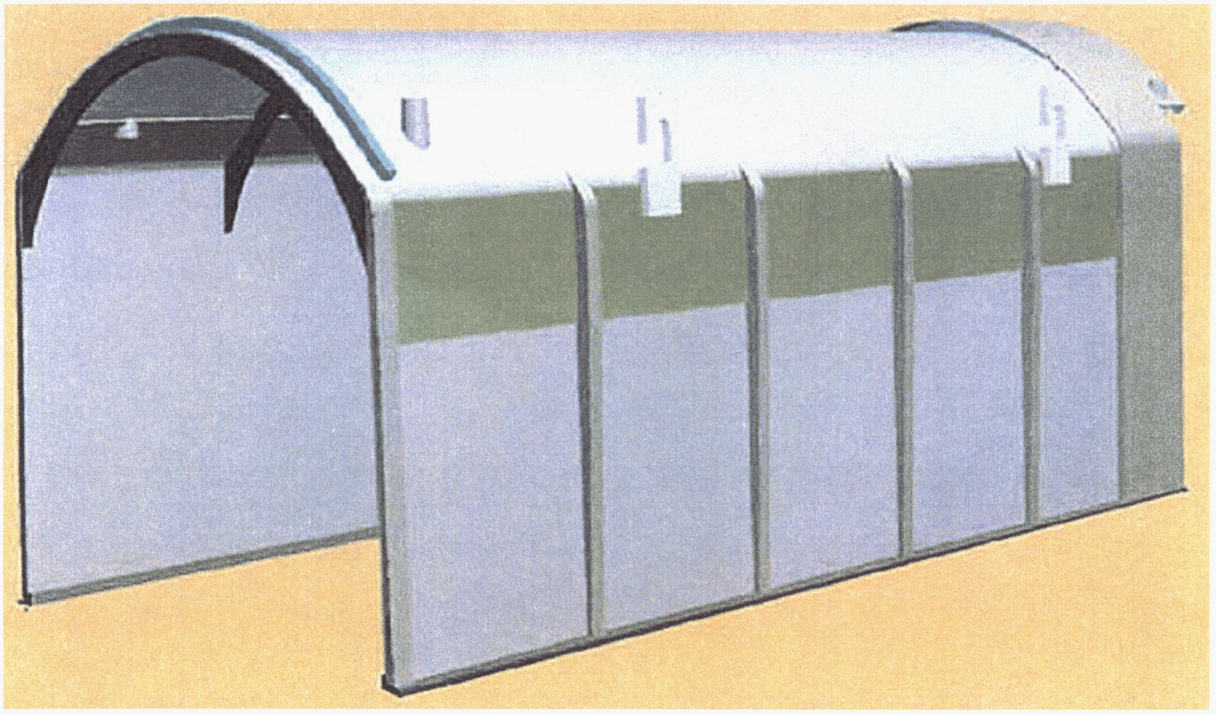

Figure 1-1. Illustration of the Drip Shield Design Proposed by the U.S. Department of Energy (Taken from Office of Civilian Radioactive Waste Management, Yucca Mountain Science and Engineering Report, DOE/RW–0539, Office of Civilian Radioactive Waste Management: North Las Vegas, Nevada, 2001)

2 FINITE ELEMENT ROCK BLOCK AND DRIP SHIELD IMPACT MODELING STUDY

This chapter documents the finite element modeling methodology used to simulate the effects of seismically induced rockfall on the drip shield. Specific modeling issues addressed are (i) individual element type used, (ii) finite element model mesh density, (iii) capabilities and limitations of the finite element code itself, (iv) various boundary conditions implemented within the model, and (v) rock block and drip shield constitutive models. The impetus behind the construction of the model is to adequately capture and quantify the amount of impact energy dissipated by way of elastic and plastic components of the drip shield deformation. The finite element model, in turn, is being used to perform a parametric study to assess the relative influence of the parameters cited in Section 1.2 of this progress report. The results presented in Chapter 3, Drip Shield and Rock Block Impact Analysis Results, demonstrate the effects that rock block size can have on the magnitude of stress and overall structural deformation experienced by the drip shield as a result of rockfall.

2.1 FINITE ELEMENT MODELING OF THE DRIP SHIELD

During the past several years, different drip shield design concepts have been considered by DOE (CRWMS M&O, 1999a,b,c; 2000b). The current drip shield design uses titanium grade 24 bulkheads and support beams as structural stiffeners for the titanium grade 7 plates. Nickel Alloy N6022 is used for the base of the drip shield to inhibit unwanted material interactions between the drip shield titanium alloys and the invert steel framework that provides the foundational support for the drip shield and waste package. Nickel Alloy N6022 is commonly referred to as Alloy 22. The relative placements of the various engineered barrier subsystem components used to construct the finite element model for the present version of the drip shield are shown in Figure 2-1 (CRWMS M&O, 2000b; 2001).

2.1.1 Drip Shield Model

Several factors must be considered when planning the proper approach for modeling the drip shield using finite element analysis methods. First and foremost is the requirement that the individual finite element type be capable of capturing all the significant physical aspects of the problem, given the boundary and load conditions to be simulated. Based on the overall thickness to length aspect ratio of the structure (i.e., approximately 0.02/5.50) the first inclination would be to use shell elements to discretize the structure. Shell element formulations within ABAQUS/Explicit (Hibbitt, Karlsson & Sorenson, Inc., 1998), however, are not intended to capture in-plane bending stresses or out of plane normal stresses relative to the shell surface. Moreover, the shell elements use reduced-integration to calculate the element internal force vector (the mass matrix and distributed loadings are still integrated exactly). Reduced-integration is used because it usually provides more accurate results for short duration dynamic events, as is the case here, and significantly reduces code execution time, especially in three dimensions. The advantages of using reduced-integration can only be achieved if the elements are not distorted or loaded by in-plane bending. Because certain parts of the structure may experience in-plane bending moments, and the out of plane normal stresses are anticipated to be significant in the area of the contact interface between the rock

block and drip shield, it was determined that shell elements are inappropriate for the task at hand.

Having ruled out the use of shell elements for discretizing the drip shield structure, the capabilities and limitations associated with using solid elements must be understood and taken into account. According to the ABAQUS/Explicit User's Manual (Hibbitt, Karlsson & Sorenson, Inc., 1998), solid continuum elements can be used for complex nonlinear analyses involving contact, plasticity, and large deformations. As with the shell elements, hexahedral (eight-node brick) solid elements are reduced-integration elements. These elements are also referred to as first-order uniform strain or centroid strain elements with hourglass control. Hourglassing occurs because reduced-integration elements consider only the linearly varying part of the incremental displacement field in the element for the calculation of the increment of physical strain. The remaining part of the nodal incremental displacement field is the hourglass field and can be expressed as hourglass modes. Excitation of these modes may lead to severe mesh distortion, with no stresses resisting the deformation. Hourglassing can be avoided by using an adequate mesh density within the model or by introducing artificial numerical damping to suppress the hourglass modes. Because the inappropriate implementation of artificial numerical damping may result in an excessively stiff response by the structure, it was decided that the problem of hourglassing would be addressed by using an adequately refined mesh.

Although much of the drip shield will experience primarily membrane stresses after impact by the rock block, bending stresses will be the dominating factor in the immediate region of the drip shield and rock block impact zone and the titanium grade 24 structural stiffeners. Because pure bending cannot be supported by a single hexahedral element (i.e., the zero-energy hourglassing mode), at least two elements must be used through the thickness of the drip shield. Having established this requirement, the second consideration is the thickness x length x width aspect ratio of the individual elements. The preferable approach is to construct the element such that the thickness, length, and width are equidistant and all vertices are 90 degrees (i.e., a perfect cube). Because the drip shield plates are modeled as 2 cm (0.787 in.) thick, each element will, to satisfy the minimum two element through the thickness requirement, have dimensions of 1 x 1 x 1 cm (0.394 x 0.394 x 0.394 in.). Given the overall dimensions of the drip shield and assuming a 1-cm^3 (0.06-in^3) volume per hexahedral element, approximately 1.12 million hexahedral elements would be required to model the entire drip shield. Modeling the drip shield with this level of refinement would require substantial computational resources and result in inordinately long execution times. To avoid this problem, it was decided that the size of the model could be significantly reduced by employing two planes of symmetry and plane strain boundary conditions (see Figure 2-2). As a final note, the rock block must impact the drip shield in a manner that maintains model symmetry. The final finite element discretization of the drip shield used for the analyses presented in this report employs 90,254, 1-cm^3 (0.061-in^3), elements with 1 x 1 x 1 (0.394 x 0.394 x 0.394 in.) aspect ratios and 128,706 nodes (see Figures 2-3a,b). Refer to Section 2.2, Finite Element Modeling of the Rock Block, for an important discussion addressing the significance of the plane strain boundary conditions and their relationship to the rock block loads used in the models.

It needs to be emphasized that when the drip shield models were being constructed the titanium grade 7 drip shield plate thickness was presumably being increased from 1.5 to 2.0 cm

(0.591 to 0.787 in.).[1] Recent DOE documents indicate, however, that the drip shield plates still have a thickness of 1.5 cm (0.591 in.) (CRWMS M&O, 2001). Consequently, the analysis results presented in this progress report underestimate the stresses incurred by the drip shield plates during rock block impacts.

2.1.2 Drip Shield Material Constitutive Models

Titanium grade 7, titanium grade 24, and Alloy 22 have been proposed for the construction of the drip shield. Alloy 22 is used for the base of the drip shield, and the bulkhead and support beam structural stiffeners are made from titanium grade 24. All other drip shield components will be fabricated using titanium grade 7. The relevant material properties for performing the drip shield and rock block impact analysis are the yield stress, modulus of elasticity, ultimate tensile strength, and the minimum required elongation. These material properties represent the minimum information needed to construct a bi-linear stress-strain curve so that the hardening behavior of the material in the plastic range can be approximated. Ideally, a stress-strain curve for the material under emplacement drift environmental conditions should be used. In the absence of qualified data meeting this requirement, the data provided by the American Society of Mechanical Engineers Boiler & Pressure Vessel Code (American Society of Mechanical Engineers, 1995, 1998) were used. As Tables 2-1 and 2-2 illustrate, the yield stress and ultimate tensile strength of titanium grade 7 are highly dependent on temperature. Note that the yield stress values for titanium grade 7 published in the 1995 and 1998 versions of the American Society of Mechanical Engineers Boiler & Pressure Vessel Code, Section II, Part D—Properties (American Society of Mechanical Engineers, 1995; 1998) are not in agreement. The yield stress and ultimate strength values presented in the 1995 and 1998 versions of the American Society of Mechanical Engineers Boiler & Pressure Vessel Code, were used to construct the bilinear stress-strain curve of titanium grade 7 for this study. Assuming the temperature of the drip shield will be 150 °C (302 °F) after emplacement within the drift, the engineering stress-strain curve can be approximated as shown in Figure 2-4. Note that the 20-percent minimum elongation in 2 in, or 50 mm as required for titanium grade 7 by the American Society for Testing and Materials Designation: B 265-98 (American Society for Testing and Materials, 1998), was assumed to be the strain corresponding to the ultimate tensile strength.

The temperature-dependent values for the yield stress, ultimate tensile strength, and Young's Modulus of titanium grade 24 are not readily available. Because the composition of titanium grade 5 and titanium grade 24 are the same except that titanium grade 24 contains 0.04- to 0.08-percent palladium, it is expected that these two grades will exhibit similar mechanical behavior (i.e., mechanical properties) and titanium grade 5 can be used as a surrogate for titanium grade 24. The Military Handbook: Metallic Materials and Elements for Aerospace Vehicle Structures (U.S. Department of Defense, 1998) and the Material Properties Handbook: Titanium Alloys (American Society for Metals International, 1994) provide extensive material data for titanium grade 5. As Table 2-3 illustrates, the values for the yield stress, ultimate strength, and Young's modulus extracted from graphical data provided in U.S. Department of Defense (1998) are also strongly dependent on temperature. Even though titanium grade 5 exhibits much higher strengths than titanium grade 7, the relative effects of temperature are still

[1]Presentation by S. Mellington at the Waste Management Symposium at Tucson, Arizona, February 27–March 2, 2000.

16/55

significant and must be considered when assessing the ability of the drip shield to withstand rock block impacts. Recalling that it has been assumed the drip shield temperature will be 150 °C (302 °F) after emplacement within the drift, the engineering stress-strain curve for titanium grade 5 can be approximated as shown in Figure 2-5. Note that the 10-percent minimum elongation in 2 in, or 50 mm as required for titanium grade 5 and titanium grade 24 by the American Society for Testing and Materials Designation: B 265-98 (American Society for Testing and Materials, 1998), was assumed to be the strain corresponding to the ultimate tensile strength.

Table 2-1. Relevant Mechanical Properties of Titanium Grade 7 as a Function of Temperature According to the 1995 American Society of Mechanical Engineers Boiler & Pressure Vessel Code

Temperature °F (°C)	Yield Stress* ksi (MPa)	Ultimate Tensile Strength† ksi (MPa)	Young's Modulus‡ ksi (GPa)
-20 to 100 (-29 to 38)	40.0 (275.8)	—	15.5×10^3 (106.9)
200 (93)	32.2 (222.0)	—	15.0×10^3 (103.4)
300 (149)	25.2 (173.8)	—	14.6×10^3 (100.7)
400 (204)	18.6 (128.2)	—	14.0×10^3 (96.5)
500 (260)	14.1 (97.2)	—	13.3×10^3 (91.7)
600 (316)	11.4 (78.6)	—	12.6×10^3 (86.9)

*1995 American Society of Mechanical Engineers Boiler & Pressure Vessel Code, Section II, Part D, Table Y–1.
† No values published.
‡1995 American Society of Mechanical Engineers Boiler & Pressure Vessel Code, Section II, Part D, Table TM–5.

17/55

Table 2-2. Relevant Mechanical Properties of Titanium Grade 7 as a Function of Temperature According to the 1998 American Society of Mechanical Engineers Boiler & Pressure Vessel Code

Temperature °F (°C)	Yield Stress* ksi (MPa)	Ultimate Tensile Strength† ksi (MPa)	Young's Modulus‡ ksi (GPa)
-20 to 100 (-29 to 38)	40.0 (275.8)	50.0 (344.8)	15.5×10^3 (106.9)
200 (93)	40.0 (275.8)	43.6 (300.6)	15.0×10^3 (103.4)
300 (149)	40.0 (275.8)	36.2 (249.6)	14.6×10^3 (100.7)
400 (204)	40.0 (275.8)	30.9 (213.1)	14.0×10^3 (96.5)
500 (260)	40.0 (275.8)	26.6 (183.4)	13.3×10^3 (91.7)
600 (316)	40.0 (275.8)	22.8 (157.2)	12.6×10^3 (86.9)

*1998 American Society of Mechanical Engineers Boiler & Pressure Vessel Code, Section II, Part D, Table Y–1.
†1998 American Society of Mechanical Engineers Boiler & Pressure Vessel Code, Section II, Part D, Table U.
‡1998 American Society of Mechanical Engineers Boiler & Pressure Vessel Code, Section II, Part D, Table TM–5.

Table 2-3. Relevant Mechanical Properties of Titanium Grade 5 as a Function of Temperature.

Temperature °F (°C)	Yield Stress* ksi (MPa)	Ultimate Tensile Strength* ksi (MPa)	Young's Modulus† ksi (GPa)
Room Temperature	120.0 (828.0)	130.0 (895.0)	16.9×10^3 (116.5)
200 (93)	105.6 (728.6)	118.3 (814.5)	16.2×10^3 (111.8)
300 (149)	94.8 (654.1)	109.2 (751.8)	15.5×10^3 (107.2)
400 (204)	85.2 (587.9)	101.4 (698.1)	14.9×10^3 (102.5)
500 (260)	78.0 (538.2)	96.2 (662.3)	14.4×10^3 (99.0)
600 (316)	74.4 (513.4)	93.6 (644.4)	13.7×10^3 (94.4)

*Room temperature reference value obtained from American Society for Testing and Materials B 265-98. Temperature correction factor extracted from Figure 5.4.1.1.1 of the "Military Handbook: Metallic Materials and Elements for Aerospace Vehicle Structures."
† Room temperature reference value obtained from Table 5.4.1.0(c_1) the temperature correction factor extracted from Figure 5.4.1.1.4 of the "Military Handbook: Metallic Materials and Elements for Aerospace Vehicle Structures."

18/55-

Table 2-4. Relevant Mechanical Properties of Alloy 22 as a Function of Temperature According to the 1998 American Society of Mechanical Engineers Boiler & Pressure Vessel Code

Temperature °F (°C)	Yield Stress* ksi (MPa)	Ultimate Tensile Strength† ksi (MPa)	Young's Modulus‡ ksi (GPa)
-20 to 100 (-29 to 38)	45.0 (310.3)	100.0 (689.5)	29.8×10^3 (205.4)
200 (93)	40.1 (276.5)	100.0 (689.5)	29.1×10^3 (200.6)
300 (149)	36.9 (254.4)	98.5 (679.1)	28.6×10^3 (197.2)
400 (204)	34.3 (236.5)	95.3 (657.1)	28.3×10^3 (195.1)
500 (260)	32.2 (222.0)	92.9 (640.5)	27.9×10^3 (192.3)
600 (316)	30.6 (211.0)	91.1 (628.1)	27.6×10^3 (190.3)

*1998 American Society of Mechanical Engineers Boiler & Pressure Vessel Code, Section II, Part D, Table Y-1.
†1998 American Society of Mechanical Engineers Boiler & Pressure Vessel Code, Section II, Part D, Table U.
‡1998 American Society of Mechanical Engineers Boiler & Pressure Vessel Code, Section II, Part D, Table TM-4 (Nickel Alloy N06455).

Because the drip shield is expected to experience large deformations and inelastic strains as a result of the rock block impact, the ABAQUS/Explicit finite element program requires that the engineering or nominal stress be converted to true stress (Cauchy stress) and the engineering or nominal strain to logarithmic strain (Hibbitt, Karlsson & Sorensen, Inc., 1998). The true stress-logarithmic strain curves used for titanium grade 7 and titanium grade 5 (i.e., titanium grade 24) in the analyses are illustrated in Figures 2-6 and 2-7. The equations used to calculate the conversions are

$$\sigma_{true} = \sigma_{nom}\left(1+\varepsilon_{nom}\right) \tag{2-1}$$

$$\varepsilon_{ln}^{pl} = \ln\left(1+\varepsilon_{nom}\right) - \frac{\sigma_{true}}{E} \tag{2-2}$$

where

σ_{true} — true stress (Cauchy stress)
σ_{nom} — nominal stress (engineering stress)
ε_{ln}^{pl} — logarithmic plastic strain
ε_{nom} — nominal strain (engineering strain)
E — Young's modulus

The ABAQUS/Explicit classical metal plasticity constitutive model is used to represent the behaviors of titanium grade 7 and titanium grade 24. Options provided with this model are the Mises or Hill yield surfaces, which allow for isotropic and anisotropic yield, respectively. Because it is assumed that the yield surfaces of the titanium alloys will behave in an isotropic manner, the Mises yield surface was used. Isotropic hardening implies that the yield surface changes size uniformly in all directions such that the yield stress increases in all stress directions as plastic straining occurs. The classical metal plasticity constitutive model also employs an associated plastic flow rule. That is, as the material yields, the inelastic deformation rate is in the direction of the normal to the yield surface. A ramification of the associated plastic flow rule in the context of classical metal plasticity is that the material will maintain a constant volume while undergoing plastic deformation (i.e., plastic deformation is volume invariant). In addition, for high-energy dynamic events, the effects of strain rate may be important. As strain rates increase, many materials show an increase in yield strength. This effect becomes important in many metals when the strain rates range between 0.1 and 1.0 per second; and it can be particularly important for strain rates ranging between 10 and 100 per second. At the present time, it is assumed that the behavior of the titanium alloys is not dependent on strain rate. One final option available with the classical plasticity constitutive model that is not presently used but may prove beneficial in future analyses, is the ability to use shear or tensile failure criteria to remove elements from the mesh. This ability allows the model to take into account the redistribution of stresses that occur when a crack is likely to have formed without having to perform a fracture mechanics based analysis.

As shown in Table 2-4, the relevant material properties for Alloy 22 are relatively unaffected by exposure to the expected emplacement drift temperature (with respect to room temperature values). Recall that the drip shield base is made from Alloy 22. Following the same procedures used for the titanium alloys, the bilinear stress-strain curves for Alloy 22 were developed (see Figures 2-8 and 2-9).

2.2 FINITE ELEMENT MODELING OF THE ROCK BLOCK

It is generally accepted that the rock block will dissipate some of the energy associated with the impact with the drip shield by localized crushing or fracturing. What is unknown is exactly how much energy is dissipated through this mechanism. Predominant factors that affect the quantity of energy dissipated in this fashion are the magnitude and distribution of stress within the rock block, which are directly dependent on the geometry of the rock block and the ability of the rock block material to support these stresses without failing (i.e., crushing or fracturing). As presented in earlier progress reports (Gute, et al., 1999, 2000), the rock block has been assumed to have cubic, spherical, or tetrahedron geometries. Moreover, the previous constitutive models for the rock block were based on the classical metal plasticity model with a Mises yield surface and perfectly plastic flow rule and the Mohr-Coulomb model cast in terms of the Drucker-Prager yield surface formulation. It is not clear at this time, however, whether the development of a rock block finite element model that can reasonably approximate the energy dissipated by crushing or fracturing during the impact event is wholly necessary. Maintaining a constant rock block mass with an infinite material strength during the impact event will, conceptually, provide conservative results because the energy dissipated by crushing or fracturing will not be accounted. The structural stiffness of the drip shield bulkheads and support beams is, however, likely to be sufficient to cause localized failure of the rock block. This localized failure of the rock block must be explicitly accounted in the model so not to

underestimate the localized shearing of the drip shield plate near the bulkhead. To accomplish this task, the plane strain boundary conditions are not applied to the face of the rock block whose outward normal is in the same direction as the positive normal defining the x–z symmetry plane (see Figure 2-2). No other provisions for rock block material or structural failure are taken into consideration within the model (i.e., a simple linear elastic constitutive model is used to represent the mechanical behavior of the rock block mass). The specific elastic rock mass material properties used in the finite element analysis are provided in Table 2-5 (NRC, 2000c). Moreover, the finite element model of the rock block was constructed using the following simplifying assumptions: (i) a parallel-piped shaped impacting rock block; (ii) the rock block impacts the apex of the drip shield crown with only a vertical component of velocity, and (iii) the rock block is sufficiently long to assume plane strain conditions.

Assumption (iii) implies that the rock block size should be interpreted as a mass per drip shield segment length. For the purpose of this study, the drip shield segment length is defined as the distance between two planes bisecting consecutive bulkhead and support beam structural stiffener pairs. The actual drip shield segment length is approximately 1.15 m (3.77 ft). This approach to defining the design basis loads offers two distinct advantages. First, it justifies the application of the plane strain boundary conditions applied in the model, allowing for a significant reduction in the number of elements required to discretize the model. Second, and more importantly, this characterization of the design basis load facilitates using the two-dimensional rockfall estimates developed by Hsiung, et al. (2000, 2001) as input to the proposed revision of the SEISMO module within the Total-system Performance Assessment code.

Lastly, unlike the drip shield, where the use of shell elements was an option, the relative dimensions of the rock block necessitates the use of solid hexahedral elements.

Table 2-5. Elastic Material Properties Used for the Rock Block Mass

Young's Modulus* ksi (GPa)	Poisson's Ratio*	Density* lb/in^3 (kg/m^3)
4.73×10^3 (32.6)	0.21	0.098 (2,700)
* U.S. Nuclear Regulatory Commission. "Input to Repository Design and Thermal-Mechanical Effects Issue Resolution Status Report." Revision 3. Washington, DC: NRC. 2000.		

2.3 DRIP SHIELD AND ROCK BLOCK IMPACT CONDITIONS

It is shown in the last progress report (Gute, et al., 2000) that combining ground motion effects with seismically induced rockfall may have a significant influence on the response of the drip shield to the impacting rock block. In the absence of specific ground motion time histories for the repository a constant upward ground velocity of 1 m/s (3.28 ft/s) was used. It is important to note, however, that this simplified approach is not capable of capturing potential dynamic amplification effects. The details of how the ground motion effects are presently being modeled is provided in Subsection 2.3.1. Subsection 2.3.2 conveys the techniques used to model the drip shield's interactions with the rock block, supporting invert, and gantry crane rails.

2.3.1 Modeling Seismic Ground Motion Effects

It is assumed that the rock block impacting the drip shield is dislodged from the emplacement drift roof by way of seismic ground motion and has an initial vertical velocity equal to the maximum vertical velocity of the ground motion. In addition, the drip shield will have a vertical component of motion. It was assumed that the drip shield was moving vertically upward at the assumed maximum vertical ground motion velocity when the rock block makes contact.

Allowing for an initial velocity and variable fall height, the velocity of the rock block at impact with the drip shield can be shown to be

$$v_{rock} = -\left[v_o^2 + 2gh\right]^{1/2} \tag{2-3}$$

where

v_o	—	initial velocity of the rock block (vertical ground velocity)
v_{rock}	—	velocity of the rock block at the time of impact
g	—	acceleration due to gravity
h	—	fall height of the rock block

Table 7-1 of the Probabilistic Seismic Hazard Analyses for Fault Displacement and Vibratory Ground Motion at Yucca Mountain, Nevada, indicates that a peak vertical ground velocity of 0.234 m/s (0.768 ft/s) has an annual probability of exceedance equal to 10^{-4} (CRWMS M&O, 1998a). The corresponding peak horizontal ground velocity is 0.472 m/s (1.55 ft/s). These peak values refer to the maximum velocities for frequencies 100 Hz and above. It is important to recognize, however, that these peak ground velocities do not necessarily correspond to the maximum ground velocities. According to Chapter 10, Disruptive Events (CRWMS M&O, 1998b), the frequency for an earthquake that results in a vertical ground motion velocity of 5 m/s is greater than 10^{-5} over a 10,000-yr period. A vertical ground motion velocity of 5 m/s (16.4 ft/s) is recognized to be quite high, and the technical basis for use of this, or any other, value as appropriate design criterion has yet to be established (including the design basis for a seismic event with an annual probability of exceedance equal to 10^{-8}). As a consequence, until actual ground motion time histories applicable to the Yucca Mountain repository horizon have been developed, it has been assumed for the purpose of this study that the maximum vertical ground velocity is 1 m/s (3.3 ft/s). In addition, horizontal ground motion has not been included in the drip shield and rock block impact simulation.

A rock block impact velocity of 7 m/s (22.97 ft/s) has been assumed. This impact velocity corresponds to a fall height of approximately 2.45 m (8.04 ft) per Equation (2-3), which is slightly greater than the 2.26 m (7.42 ft) allowable falling distance.

Although the velocity of the rock block at the time of impact is not affected significantly by the ground motion, the interaction between the drip shield and rock block may be influenced strongly by the seismic excitation at the base of the drip shield. For structures with natural frequencies below 33 Hz, resonance can play a major role in the way the structure will respond to seismic excitation. Given a time–history representation of the seismic motion, the dynamic amplification aspects of the problem can be studied in detail. In the absence of this information,

certain simplifying assumptions must be made. At present, the ground motion is modeled by setting the vertical velocity of the entire drip shield to the assumed vertical ground motion velocity. Transient acceleration effects are removed from the system, and the drip shield is in a steady-state condition as a consequence of this approach. Then, just as the rock block impacts the drip shield, the velocities of the individual nodes of the drip shield are freed from all displacement, velocity, and acceleration constraints. Because the duration of the drip shield and rock block impact event was not known prior to performing the analyses, it was decided that the vertical ground motion may be reasonably approximated as a constant value if the duration of the event was reasonably short. A constant upward ground motion is implemented within the model by keeping constant the upward vertical velocity of the rigid analytical surface used to represent the invert and gantry rails (see Subsection 2.3.2 for additional information pertaining to the interactions between the drip shield and the aforementioned rigid analytical surface).

2.3.2 Modeling the Drip Shield Contact Interactions

Three different contact interactions are explicitly accounted for in the drip shield and rock block impact model. These are the interactions between the drip shield and the: (i) rock block, (ii) supporting invert, and (iii) adjacent gantry rail. A master–slave concept is used within the finite element program to model these interactions. Specifically, the nodes associated with the slave surface cannot penetrate into or through the master surface mesh. The master surface nodes, however, can penetrate through the slave surface. As a consequence, the slave surface mesh should be much more refined than the master surface. Another option is to redundantly define the master–slave relationship—the contact surface pair is defined twice, with the surfaces interchanging the master–slave relationship. A redundant master–slave relationship does not allow any nodes from either surface to penetrate through the counterpart surface. Even though the effects of friction can be included as part of the interaction between the two surfaces, the duration and magnitude of the impact load are such that these effects are negligible.

For the case of the drip shield and rock block interaction, the coarsely meshed rock block is used to define the master surface and the drip shield is the corresponding slave surface. No redundancy was used.

Unlike the previous progress report, where the nodes at the base of the drip shield were completely fixed to the invert, the new model reflects that the drip shield is a free-standing structure on the invert. In particular, the new model employs friction free sliding contact boundary conditions between the drip shield and the rigid analytical surface that is used to represent the invert and gantry rails (see Figure 2-3). Note that the gantry rail (i.e., the vertical side of the rigid analytical surface) limits the horizontal deflections of the drip shield and provides a potential pivot point to cause the drip shield to fold up underneath itself (i.e., buckle) if the deformations were to become sufficiently large. As with the drip shield and rock block interaction, no redundancy was used in modeling the interaction between the drip shield and the rigid analytical surface.

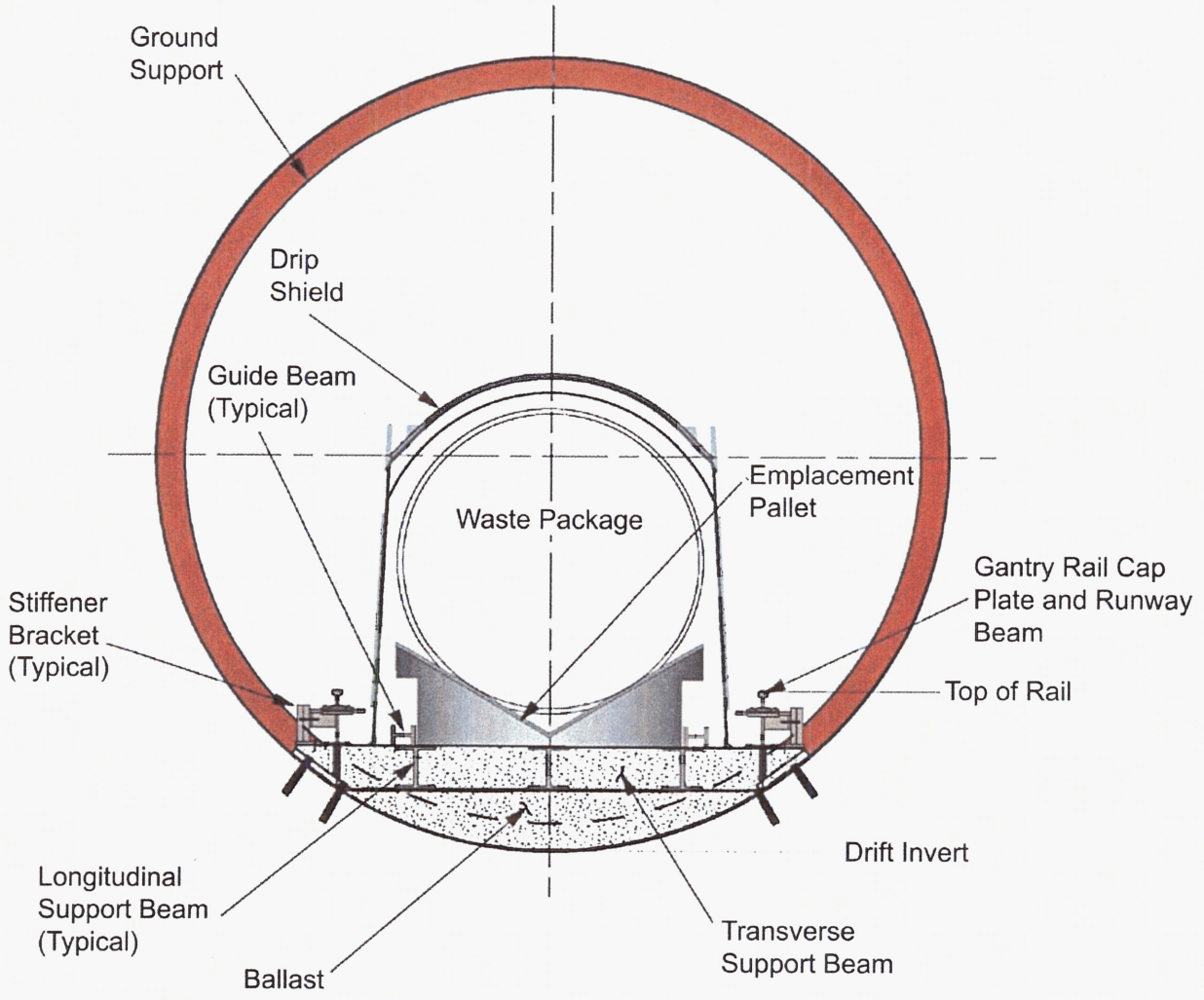

Figure 2-1. Schematic of the Proposed Engineered Barrier Subsystem (Taken from Office of Civilian Radioactive Waste Management, Yucca Mountain Science and Engineering Report, DOE/RW–0539, Office of Civilian Radioactive Waste Management: Las Vegas, Nevada, 2001)

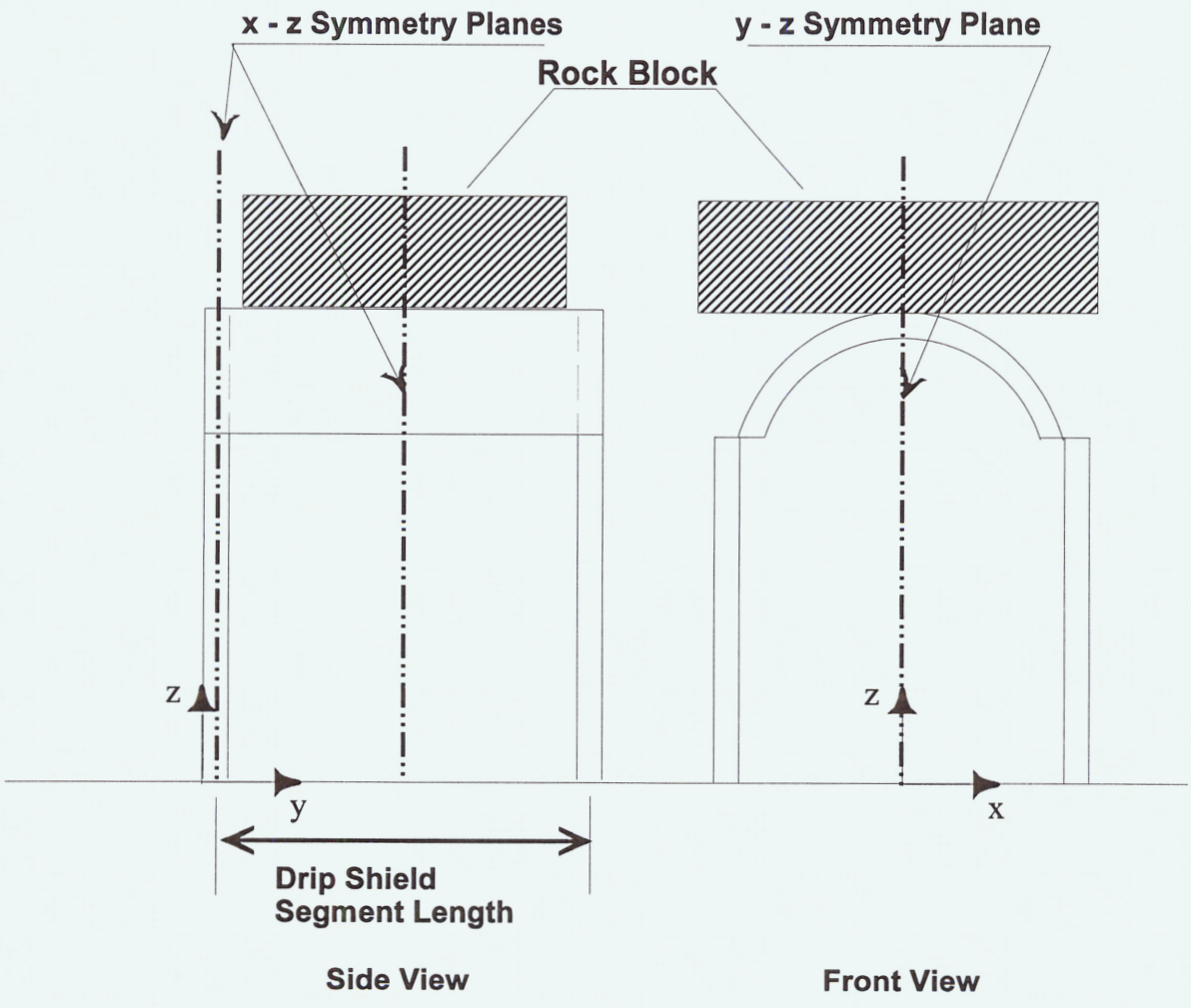

Figure 2-2. Schematic Illustrating the Symmetry Planes Used to Simplify the Finite Element Model

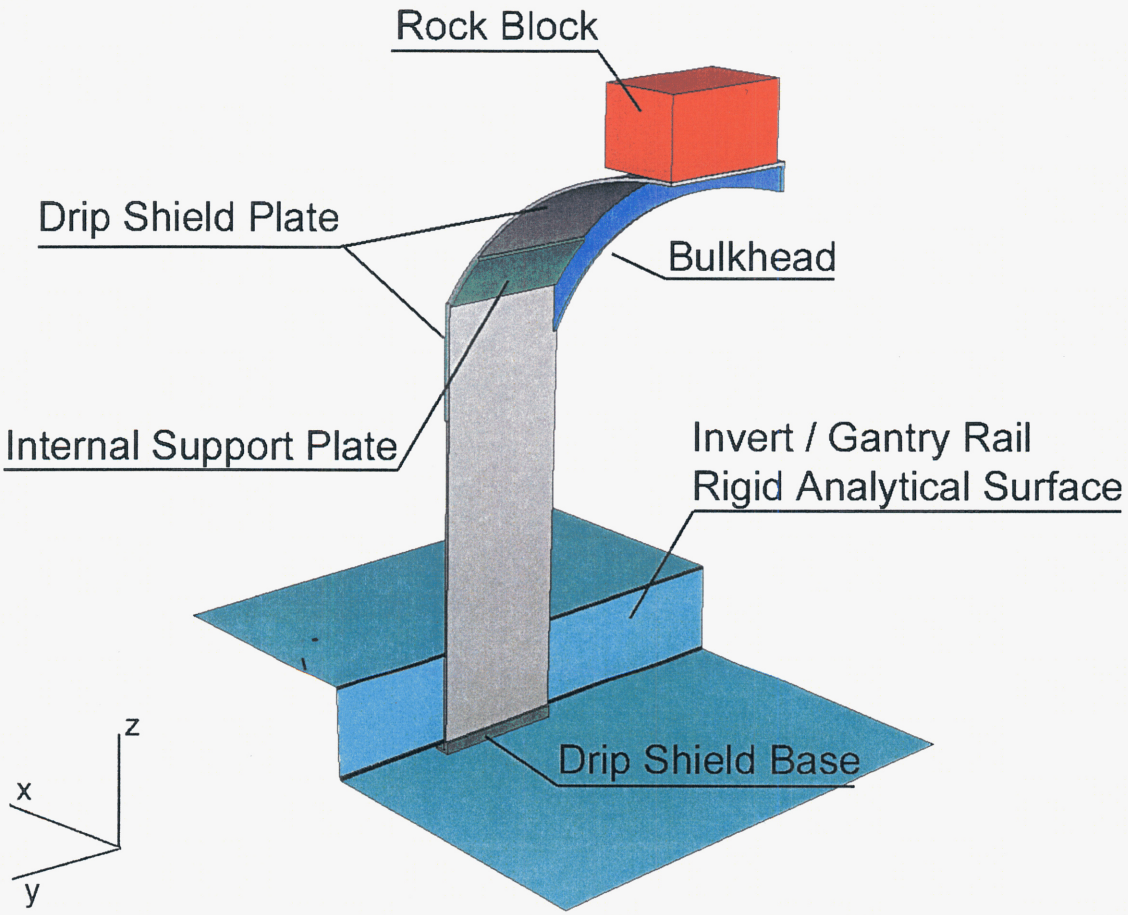

Figure 2-3a. Drip Shield–Rock Block Impact Finite Element Model

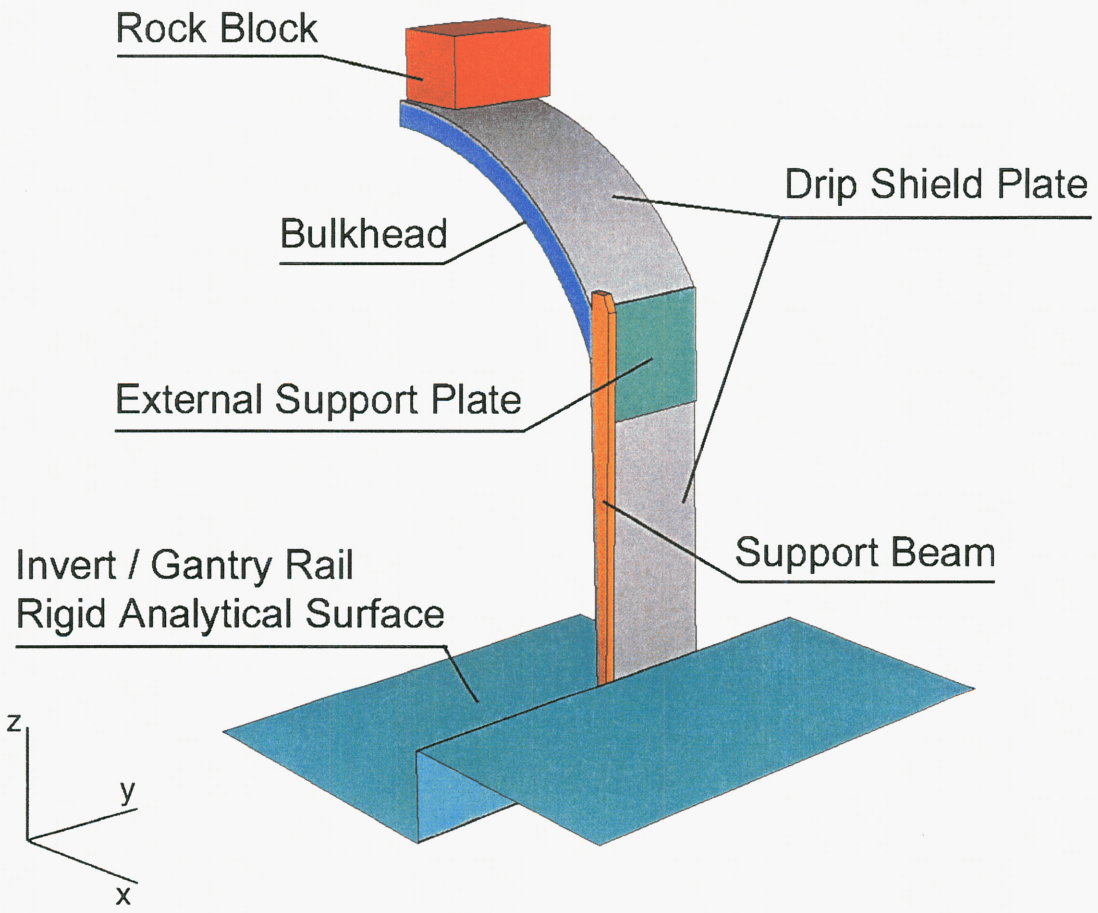

Figure 2-3b. Drip Shield–Rock Block Impact Finite Element Model

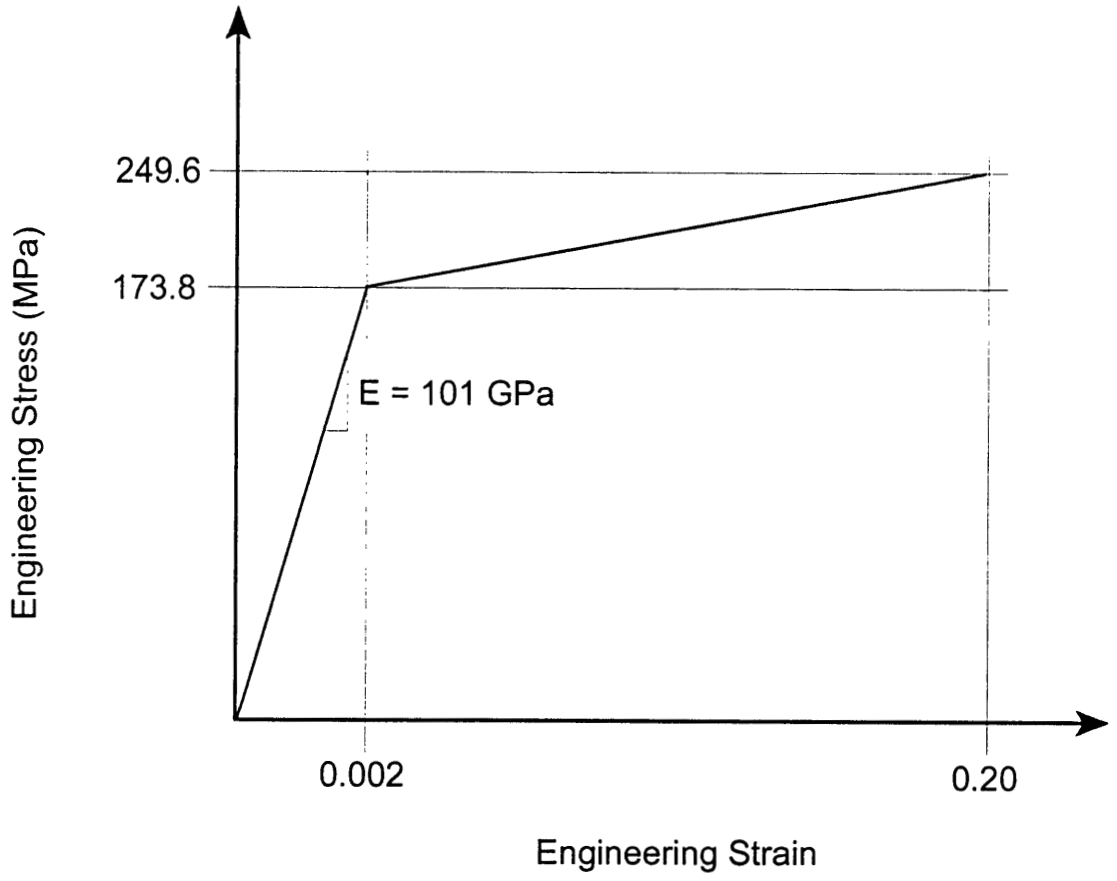

Figure 2-4. Schematic of the Engineering Stress–Engineering Strain Curve for Titanium Grade 7 at 150 °C (302 °F)

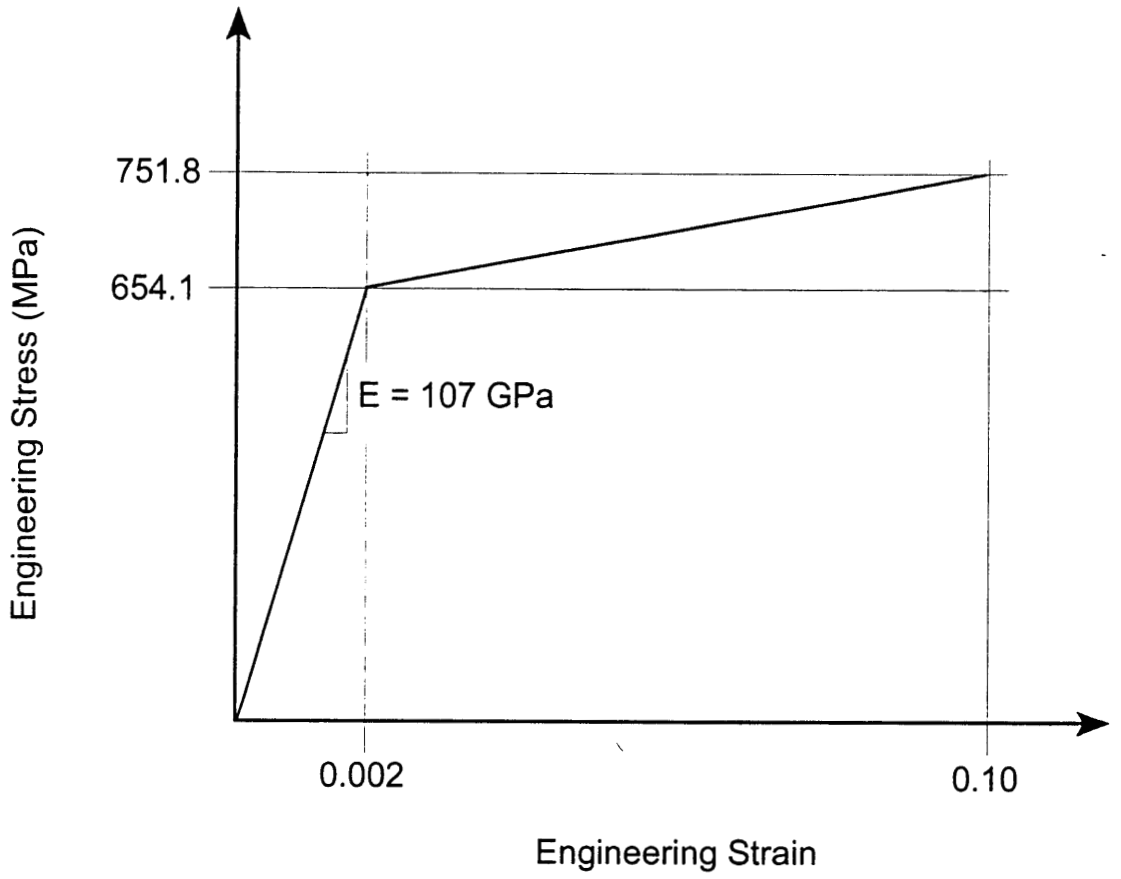

Figure 2-5. Schematic of the Engineering Stress–Engineering Strain Curve for Titanium Grades 5 and 24 at 150 °C (302 °F)

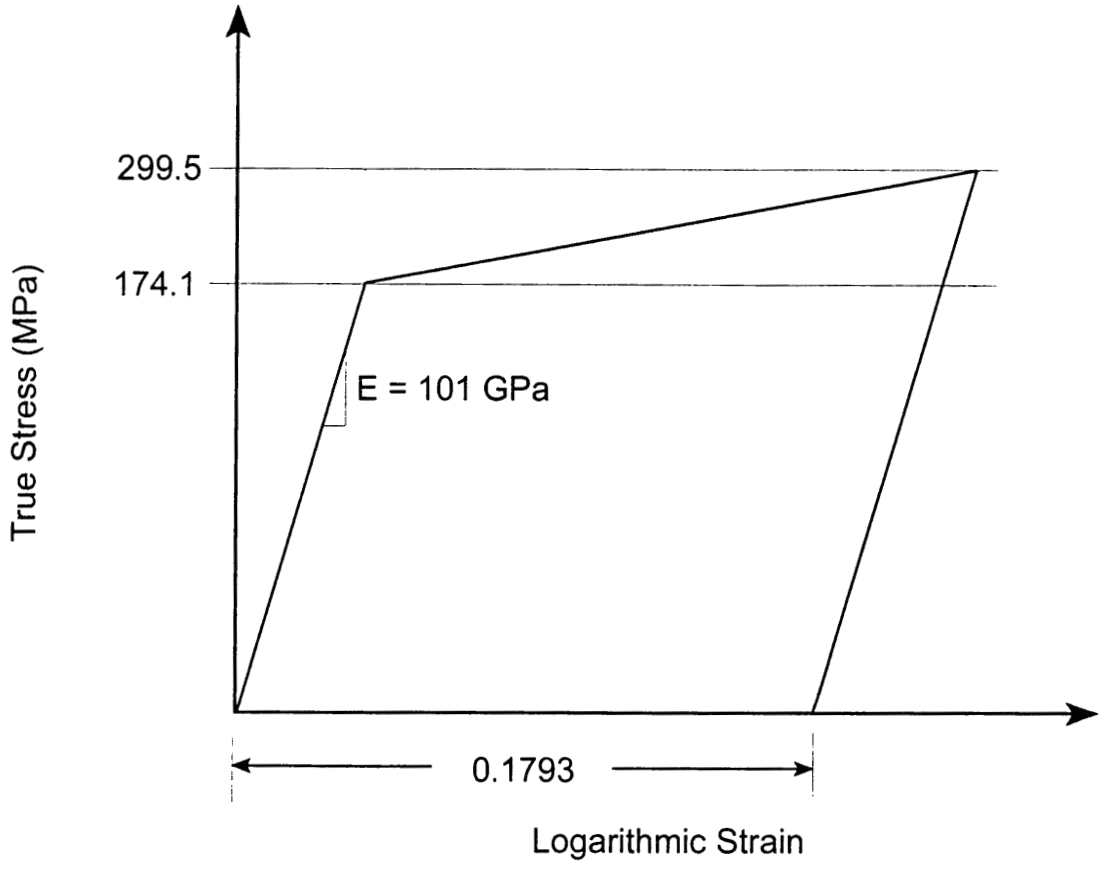

Figure 2-6. Schematic of the True Stress–Logarithmic Strain Curve for Titanium Grade 7 at 150 °C (302 °F)

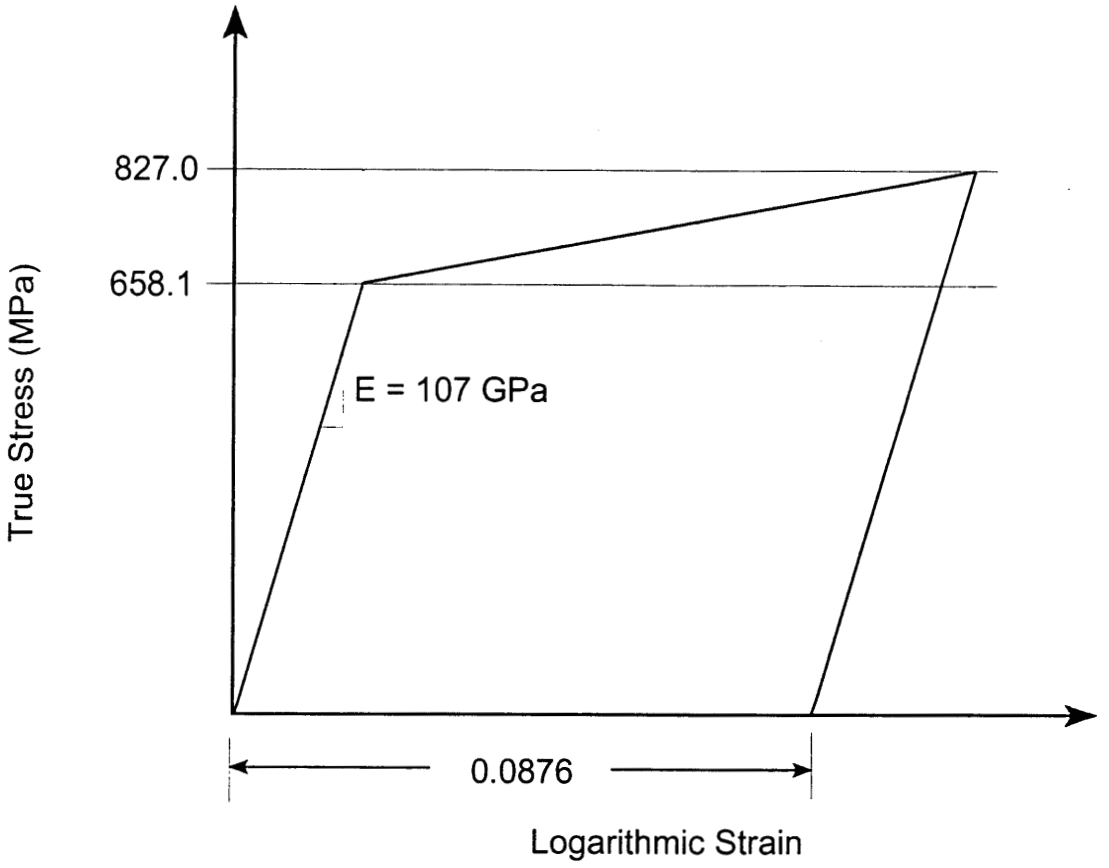

Figure 2-7. Schematic of the True Stress–Logarithmic Strain Curve for Titanium Grades 5 and 24 at 150 °C (302 °F)

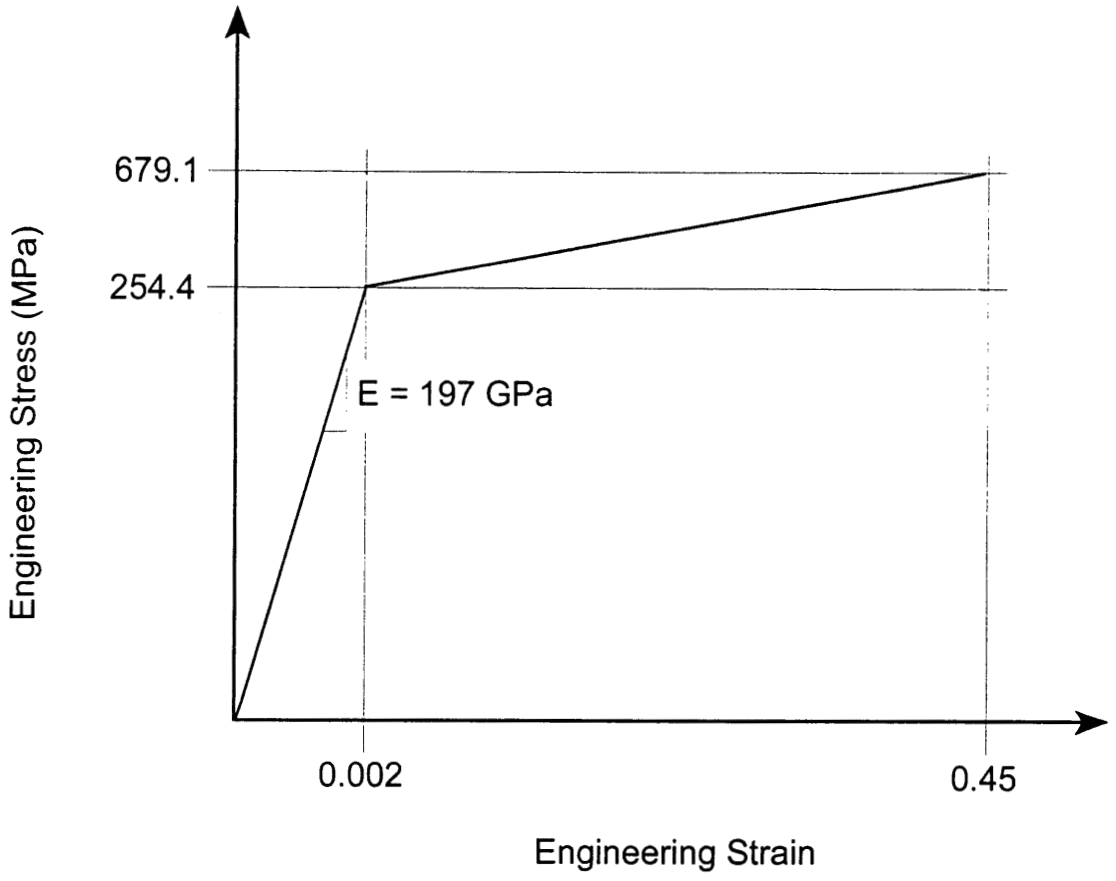

Figure 2-8. Schematic of the Engineering Stress–Engineering Strain Curve for Alloy 22 at 150 °C (302 °F)

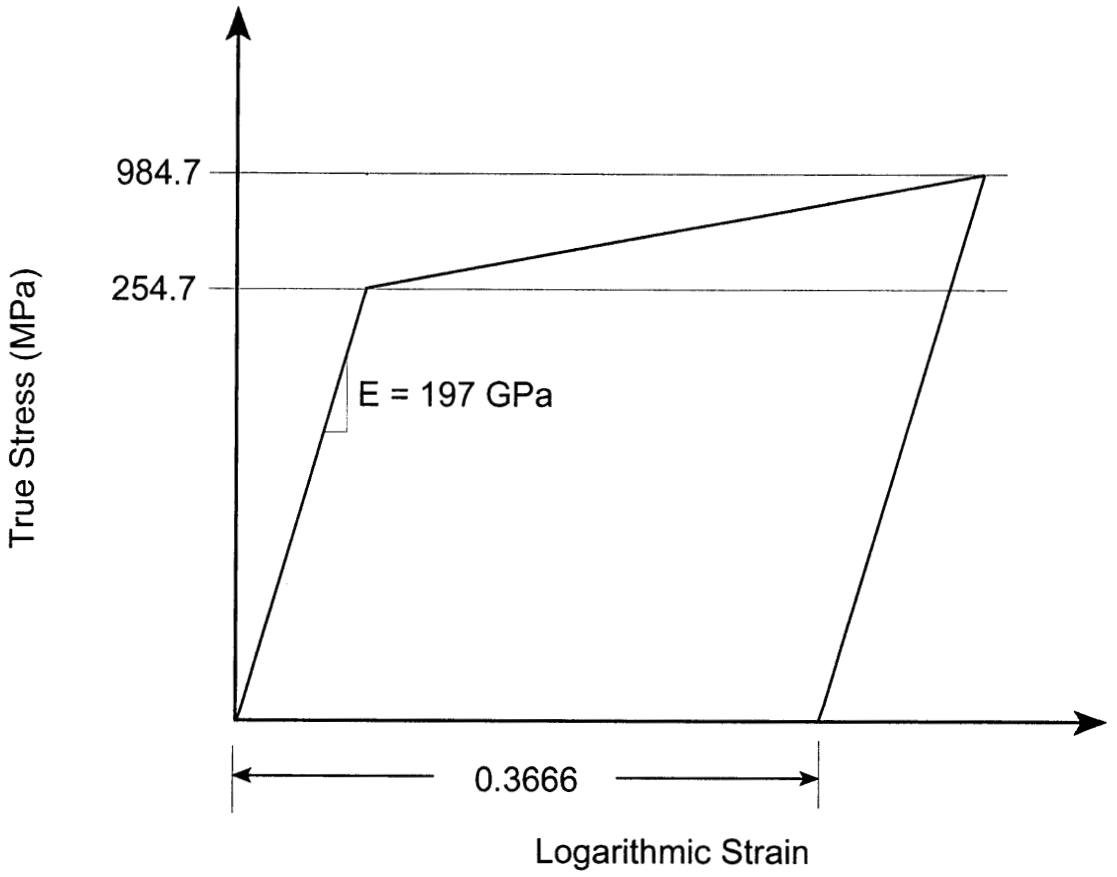

Figure 2-9. Schematic of the True Stress–Logarithmic Strain for Alloy 22 at 150 °C (302 °F)

3 DRIP SHIELD AND ROCK BLOCK IMPACT ANALYSIS RESULTS

Before presenting the simulation results it must be reiterated that the finite element model was constructed using the approximations and assumptions described in Chapter 2. In addition, the drip shield structure was modeled using the dimensions provided in CRWMS M&O (2000c), with the notable exception of using 2-cm (0.787-in.) thick titanium grade 7 plates instead of 1.5-cm (0.591-in.) plates.

The drip shield and rock block impact analyses were performed for three different cases: 0.5-, 1.0-, and 2.0-tonne (1,102-, 2,205-, and 4,409-lb) rock block sizes per drip shield segment length. As can be seen in Figure 3-1, which is a plot of the drip shield crown displacement relative to the bottom of the drip shield base as a function of the elapsed time after the rock block impact, the drip shield deflections can be quite large, even for relatively small rock block sizes. According to the dimensions provided in CRWMS M&O (2000b), the clearances between the drip shield and different waste package types vary in the range 0.080–0.592 m (3.15–23.3-in.). Specific drip shield and waste package clearances are tabulated in Table 3-1. Figure 3-1 clearly shows that rock blocks characterized as greater than 1.0 tonne per drip shield segment length are sufficient to drive the drip shield into the defense high-level waste package.

It was also observed in all three cases that the elastic energy remaining in the drip shield after reaching the initial maximum displacement was still sufficient to launch the impacting rock block back into the air. In fact, the drip shield base was seen to jump up off of the invert surface while launching the impacting rock block back into the air. Furthermore, the oscillations in the displacements seen in Figure 3-1 after the drip shield and rock block are no longer in contact occur because the drip shield is structurally ringing or vibrating because some of its resonant frequencies have been excited by the rock block impact.

Table 3-1. Clearances Between the Drip Shield and Different Waste Package Types

Waste Package Type	Drip Shield–Waste Package Clearance* in. (m)
Defense High-Level Waste	3.15 (0.080)
Naval	10.0 (0.254)
44-Boiling Water Reactor	22.0 (0.559)
21-Pressure Water Reactor	23.3 (0.592)

*CRWMS M&O. Design Analysis for the Ex-Container Components. ANL–XCS–ME–000001. Revision 00. Las Vegas, Nevada: CRWMS M&O. 2000.

Additional results obtained from the finite element analyses of the drip shield and rock block impact problem are the level of stresses experienced by the different drip shield components (i.e., the titanium grade 7 plates and titanium grade 24 bulkhead and support beam structural stiffeners during the impact event). Figures 3-2 through 3-4, for example, illustrate the Von Mises stress magnitudes and distributions corresponding to the maximum drip shield

deflections created by 0.5-, 1.0-, and 2.0-tonne (1,102-, 2,205-, and 4,409-lb) rock block impacts per drip shield segment length. Recall that Von Mises stress is the equivalent uniaxial stress that causes the same distortion energy as the generalized three-dimensional stress state the material is actually subjected to [i.e., the energy associated with changes in shape (as opposed to the energy associated with changes in volume)]. According to the Von Mises yield criterion, a given structural component will not experience plastic deformations if the maximum value of the distortion energy per unit volume in the material remains smaller than the distortion energy per unit volume required to cause yield in a tensile-test specimen of the same material. Note that the energy associated with changes in volume for most metals is not considered because material yielding has been observed to be unaffected by the magnitude of the dilatational (i.e., hydrostatic) volume changing stress. The Von Mises stress does not exceed the titanium grade 24 yield stress of 658.1 Mpa (25.3-ksi) in the bulkhead or support beam for the 0.5-tonne (1,102-lb) per drip shield segment length impact load. The 1.0- and 2.0-tonne (2,205-, and 4,409-lb) rock block impact per drip shield segment length loads, on the other hand, indicate that the bulkhead stress level has exceeded the titanium grade 24 yield stress (see Figures 3-3 and 3-4). And, in the case of the 2.0-tonne (4,409-lb) per drip shield segment length impact load, the support beam has also experienced Von Mises stresses beyond the titanium grade 24 yield stress.

Because the 174.1-MPa (25.3 ksi) yield stress for the titanium grade 7 is significantly smaller than the 658.1 MPa (95.5 ksi) for titanium grade 24, the Von Mises stresses for the titanium grade 7 drip shield plate has to be plotted separately with a more appropriate scale to assess the magnitude of the damage, if any, it may be experiencing. Referring to Figures 3-5 through 3-7, it can be seen that, even for the 0.5-tonne (1,102-lb) rock block case, the titanium grade 7 yield stress has been exceeded. It needs to be reiterated that the drip shield plate has been modeled with a 2-cm (0.787-in.) thickness, not the 1.5-cm (0.591-in.) thickness defined in recent DOE documents. The stress levels in the drip shield plate have been underestimated as a result.

Drip shield components subjected to Von Mises stress magnitudes greater than this material's yield stress have incurred some plastic deformation and may be susceptible to stress corrosion cracking because of the residual stresses remaining after the impact event. Because of the high strain rates associated with a rock block impact, however, the amount of yielding predicted by the finite element models may have been overestimated. Recall that high strain rates typically increase the effective yield stress of most metals. Moreover, none of the cases evaluated resulted in Von Mises stress magnitudes that exceeded the ultimate strength of titanium grade 7 or titanium grade 24, which would be indicative of the drip shield being breached. It needs to be emphasized, however, that the sizes of the impacting rock blocks evaluated thus far are considered to be relatively small.

It is interesting to note that the maximum stresses experienced by the individual drip shield components do not necessarily occur at the same time as the maximum deflection. This result can be attributed to the stress pulse created by the initial impact propagating through the drip shield structure. Figures 3-8 through 3-16 show the maximum Von Mises stress levels predicted by the finite element models for the drip shield bulkhead, support beam, and plate for each rock block impact case. For all three cases, the maximum Von Mises stress for the bulkhead and plate exceeded the yield stress of the respective materials. The maximum Von Mises stress for the support beam exceeded the yield stress only in the case of the 2-tonne (4,409-lb) rock block impact per drip shield segment length.

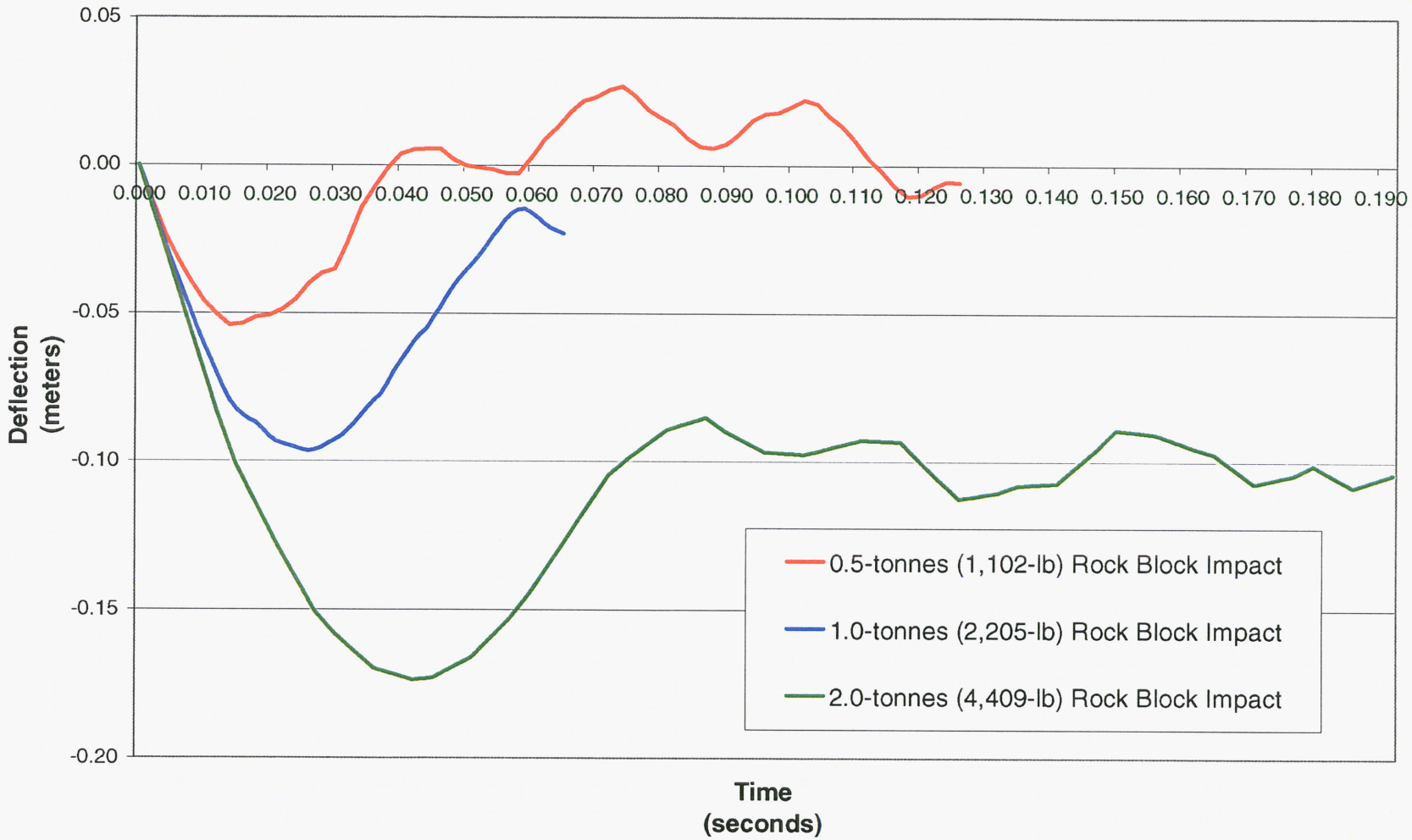

Figure 3-1. Drip Shield Deflections for Various Rock Block Impact Cases

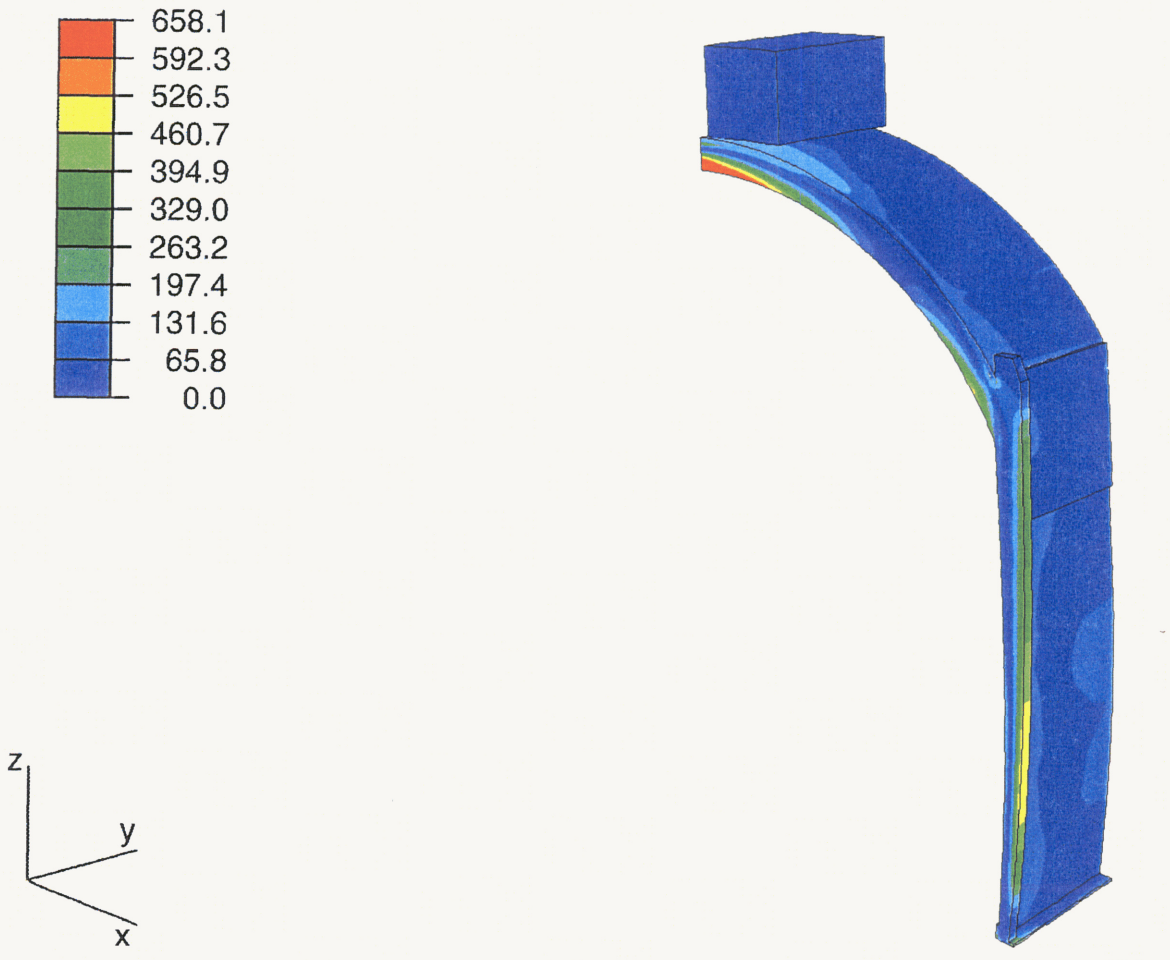

Figure 3-2. Von Mises Stress (MPa) Distribution in the Drip Shield at the Maximum Deflection Point Due to a 0.5-tonne (1,102-lb) Rock Block Impact per Drip Shield Segment Length

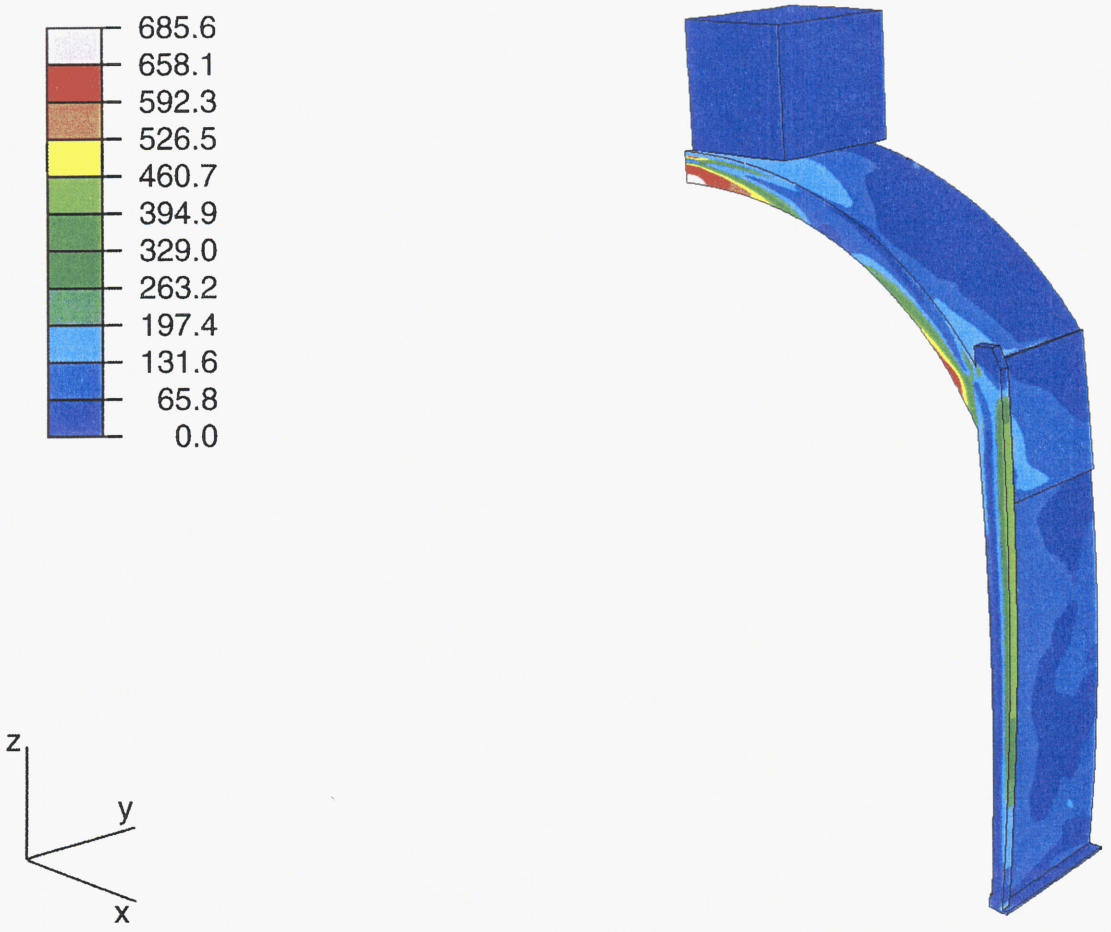

Figure 3-3. Von Mises Stress (MPa) Distribution in the Drip Shield at the Maximum Deflection Point Due to a 1.0-tonne (2,205-lb) Rock Block Impact per Drip Shield Segment Length

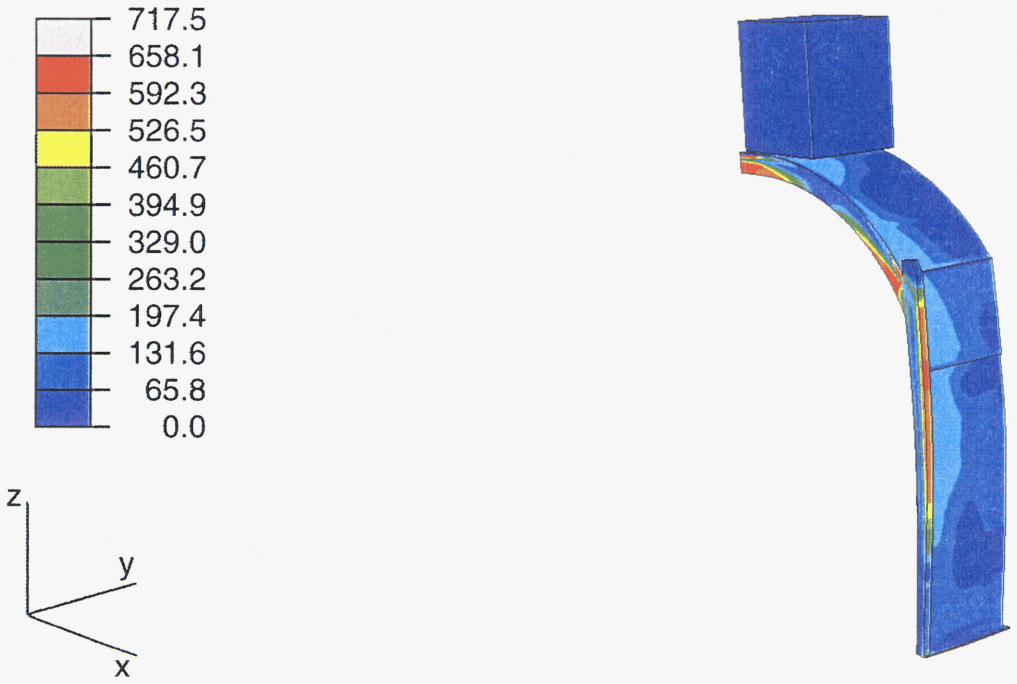

Figure 3-4. Von Mises Stress (MPa) Distribution in the Drip Shield at the Maximum Deflection Point due to a 2.0-tonne (4,409-lb) Rock Block Impact per Drip Shield Segment Length

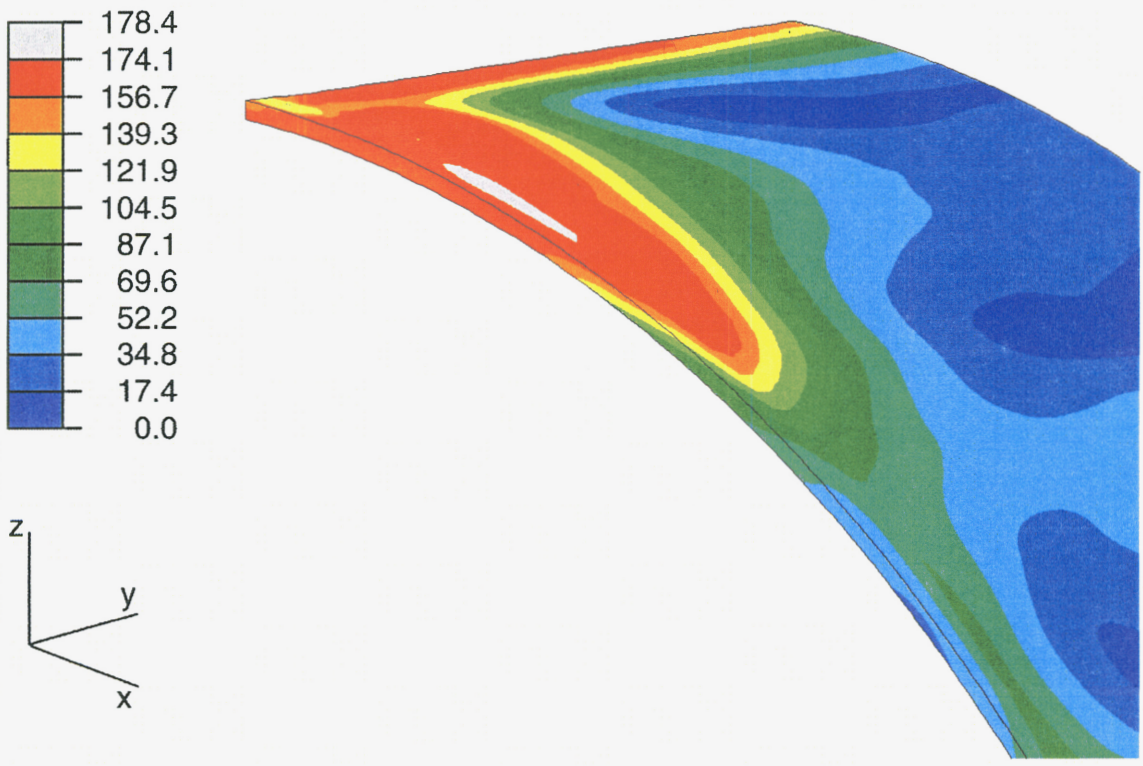

Figure 3-5. Von Mises Stress (MPa) Distribution in the 2-cm (0.787-in.) Thick Titanium Grade 7 Drip Shield Plate at the Maximum Deflection Point due to a 0.5-tonne (1,102-lb) Rock Block Impact per Drip Shield Segment Length

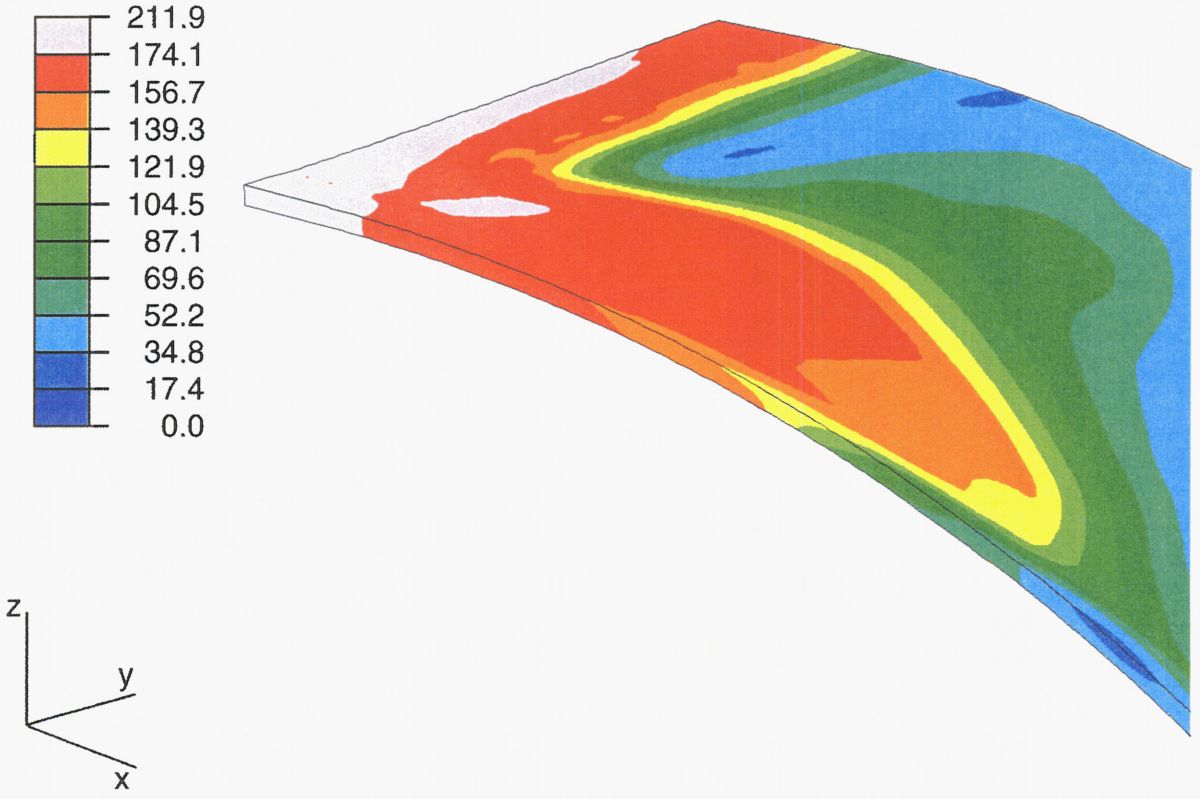

Figure 3-6. Von Mises Stress (MPa) Distribution in the 2-cm (0.787-in.) Thick Titanium Grade 7 Drip Shield Plate at the Maximum Deflection Point due to a 1.0-tonne (2,205-lb) Rock Block Impact per Drip Shield Segment Length

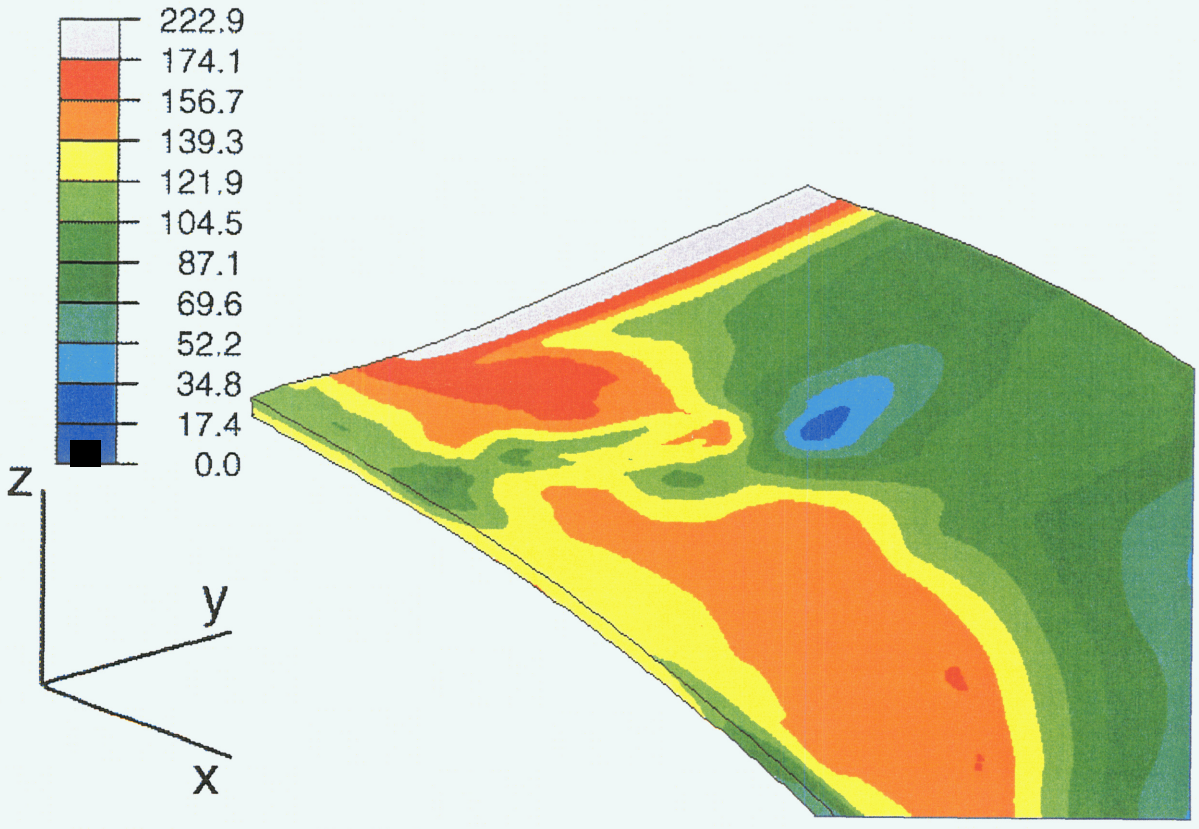

Figure 3-7. Von Mises Stress (MPa) Distribution in the 2-cm (0.787-in.) Thick Titanium Grade 7 Drip Shield Plate at the Maximum Deflection Point due to a 2.0-tonne (4,409-lb) Rock Block Impact per Drip Shield Segment Length

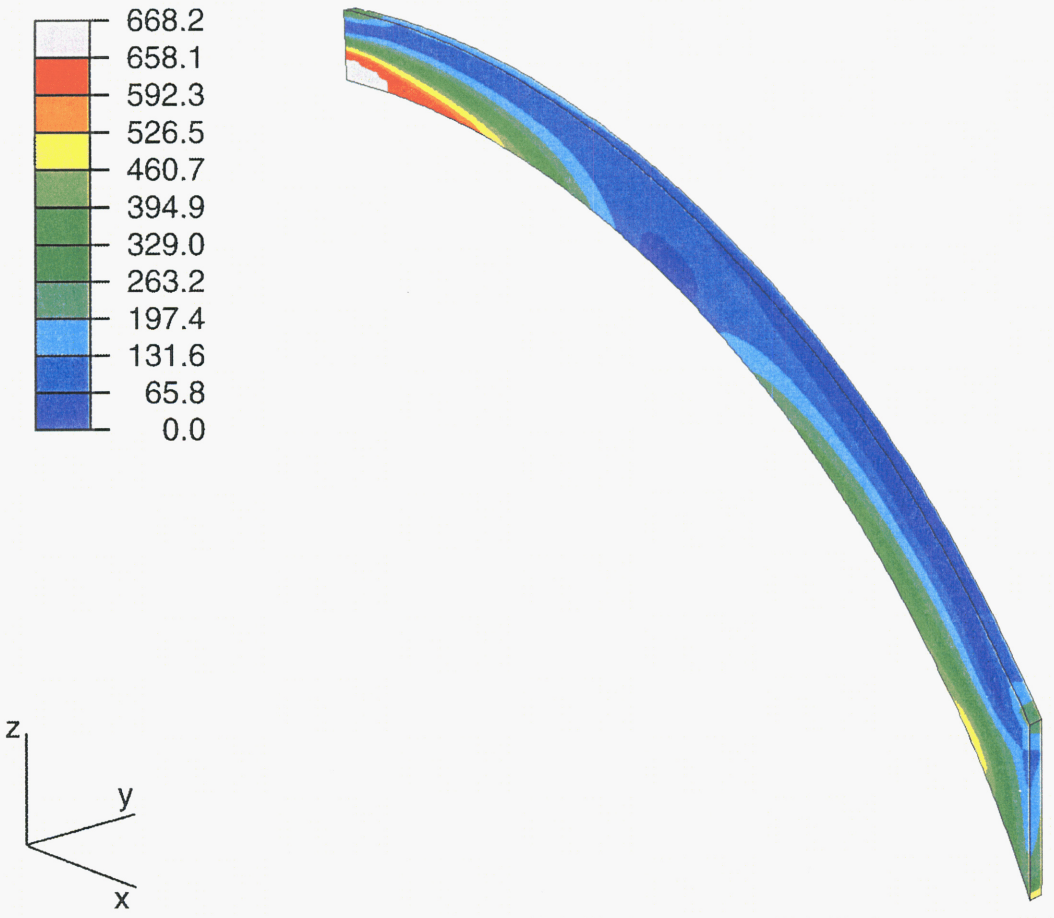

Figure 3-8. Maximum Von Mises Stress (MPa) Level Incurred by the Drip Shield Bulkhead due to a 0.5-tonne (1,102-lb) Rock Block Impact per Drip Shield Segment Length

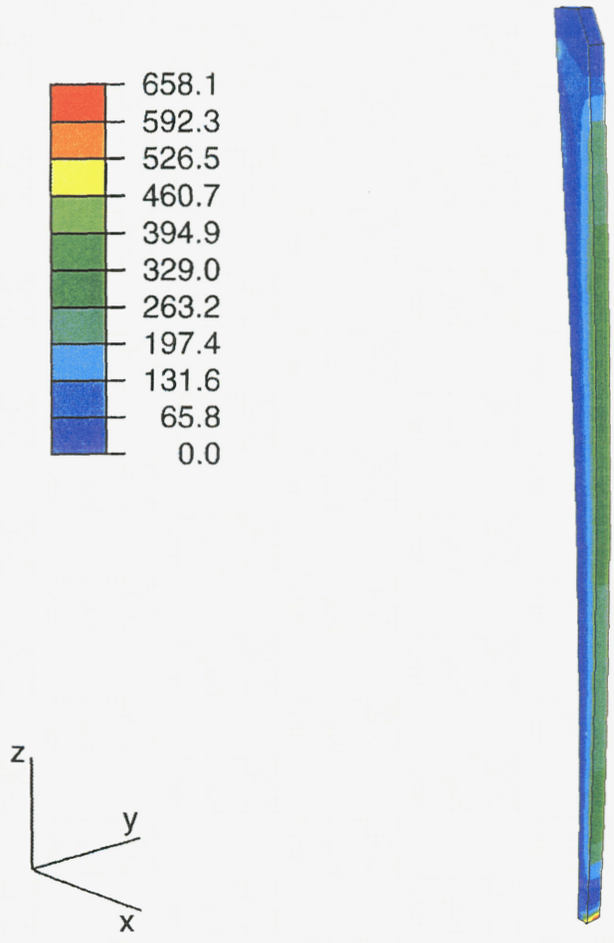

Figure 3-9. Maximum Von Mises Stress (MPa) Level Incurred by the Drip Shield Support Beam due to a 0.5-tonne (1,102-lb) Rock Block Impact per Drip Shield Segment Length

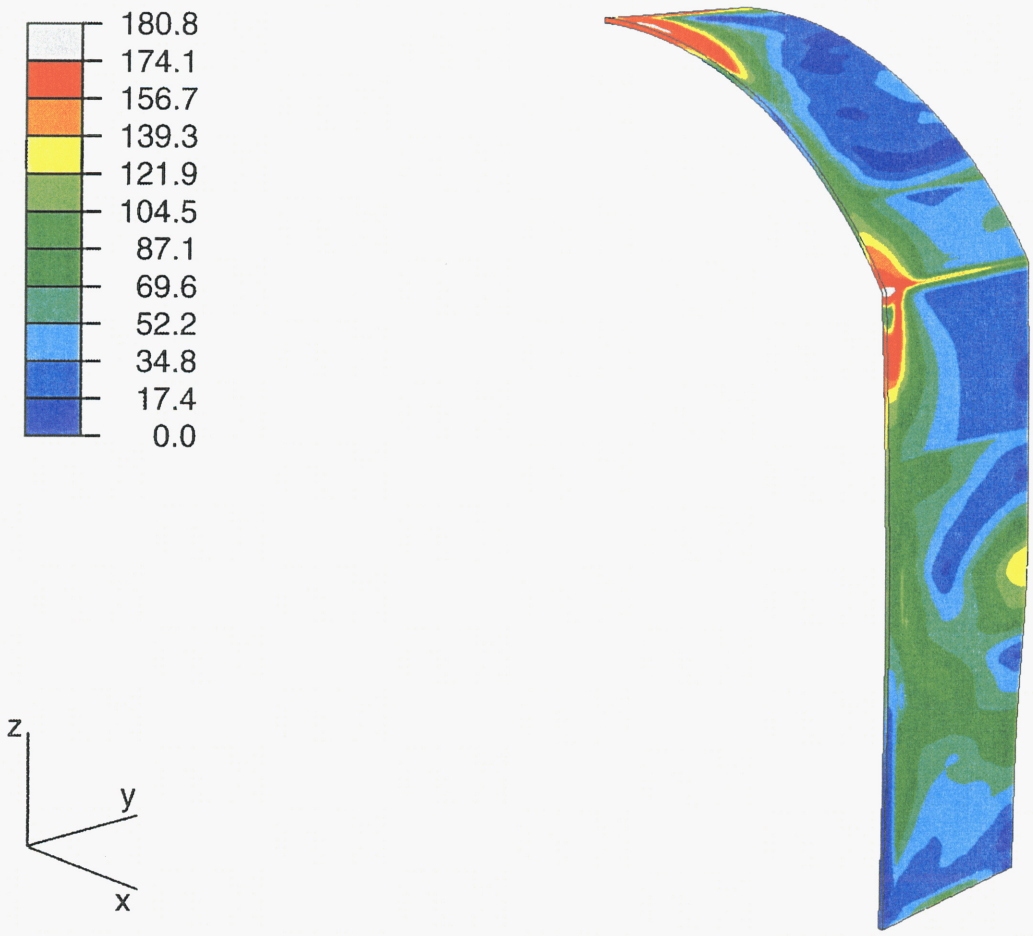

Figure 3-10. Maximum Von Mises Stress (MPa) Level Incurred by the 2-cm (0.787-in.) Thick Drip Shield Plate due to a 0.5-tonne (1,102-lb) Rock Block Impact per Drip Shield Segment Length

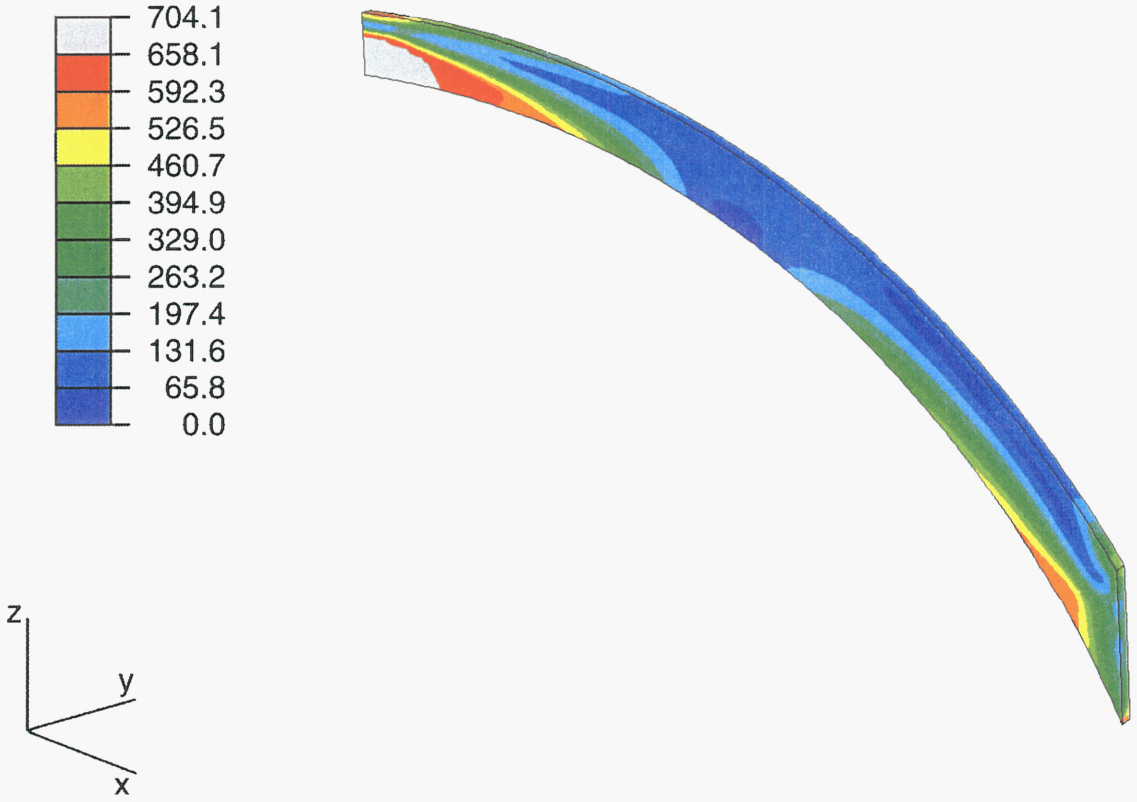

Figure 3-11. Maximum Von Mises Stress (MPa) Level Incurred by the Drip Shield Bulkhead due to a 1.0-tonne (2,205-lb) Rock Block Impact per Drip Shield Segment Length

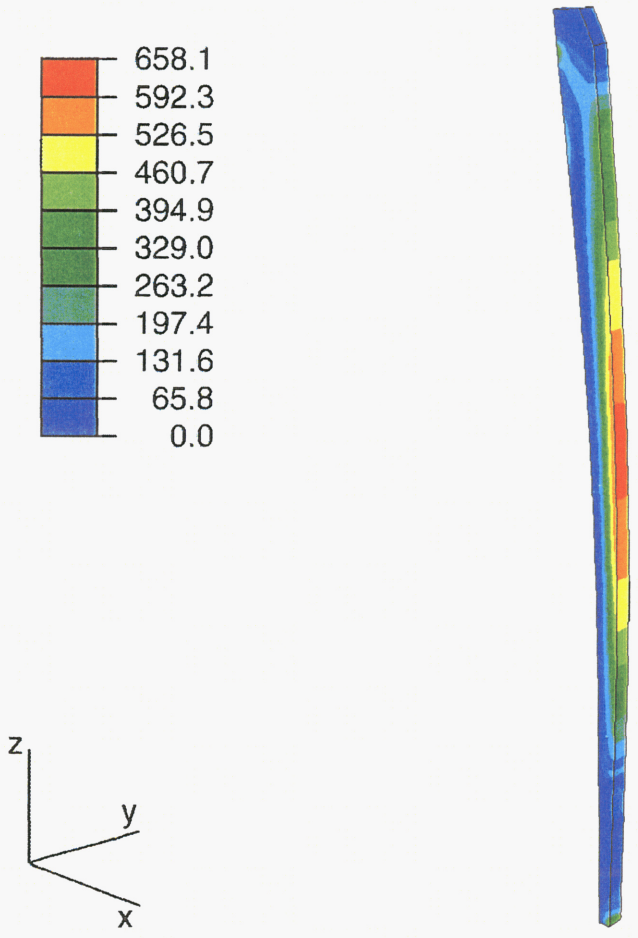

Figure 3-12. Maximum Von Mises Stress (MPa) Level Incurred by the Drip Shield Support Beam due to a 1.0-tonne (2,205-lb) Rock Block Impact per Drip Shield Segment Length

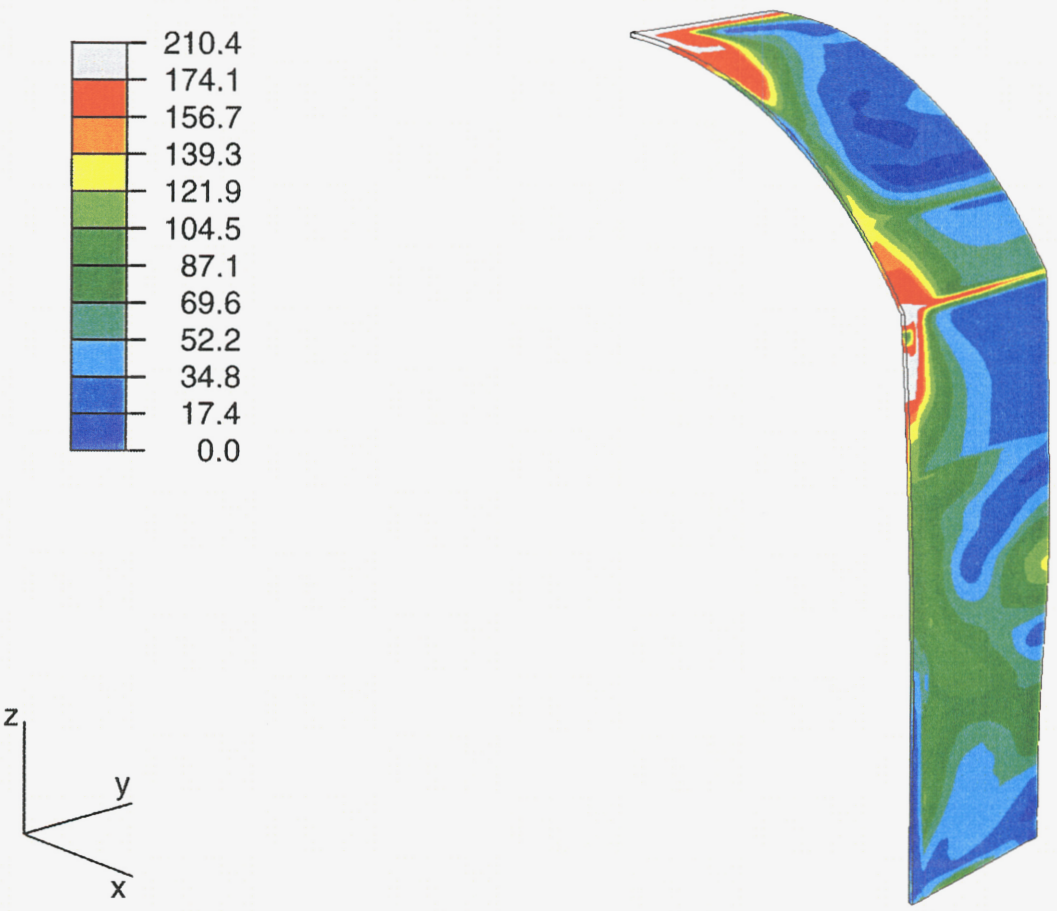

Figure 3-13. Maximum Von Mises Stress (MPa) Level Incurred by the 2-cm (0.787-in.) Thick Drip Shield Plate due to a 1.0-tonne (2,205-lb) Rock Block Impact per Drip Shield Segment Length

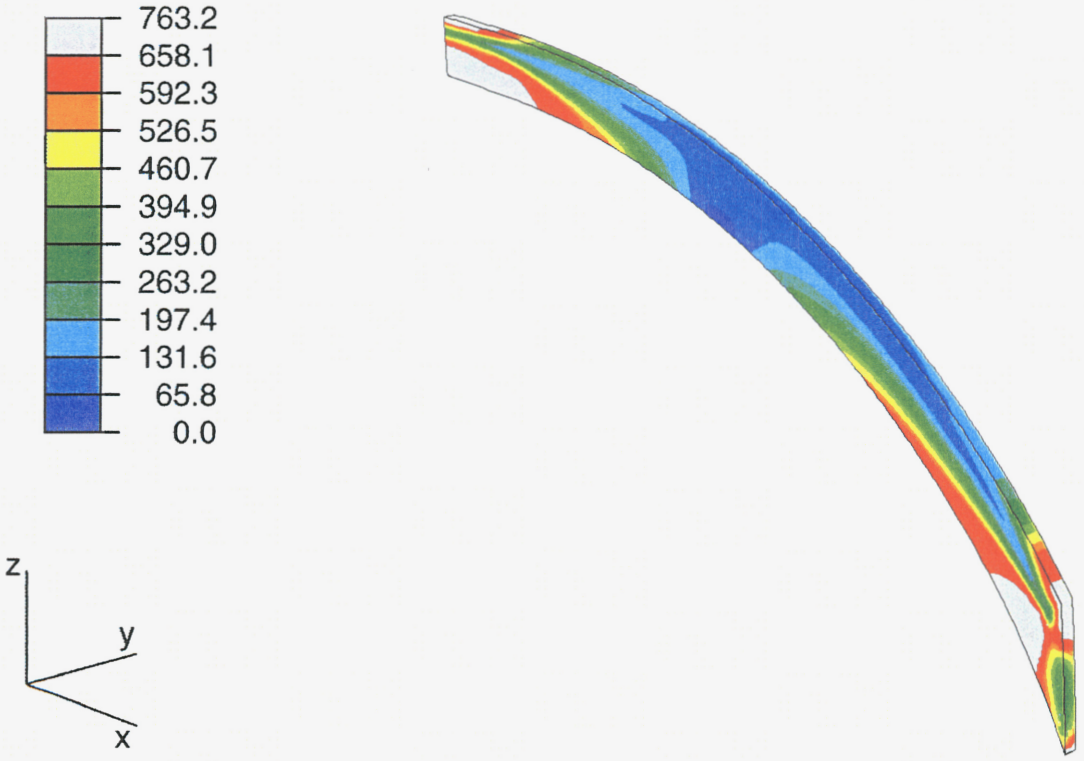

Figure 3-14. Maximum Von Mises Stress (MPa) Level Incurred by the Drip Shield Bulkhead due to a 2.0-tonne (4,409-lb) Rock Block Impact per Drip Shield Segment Length

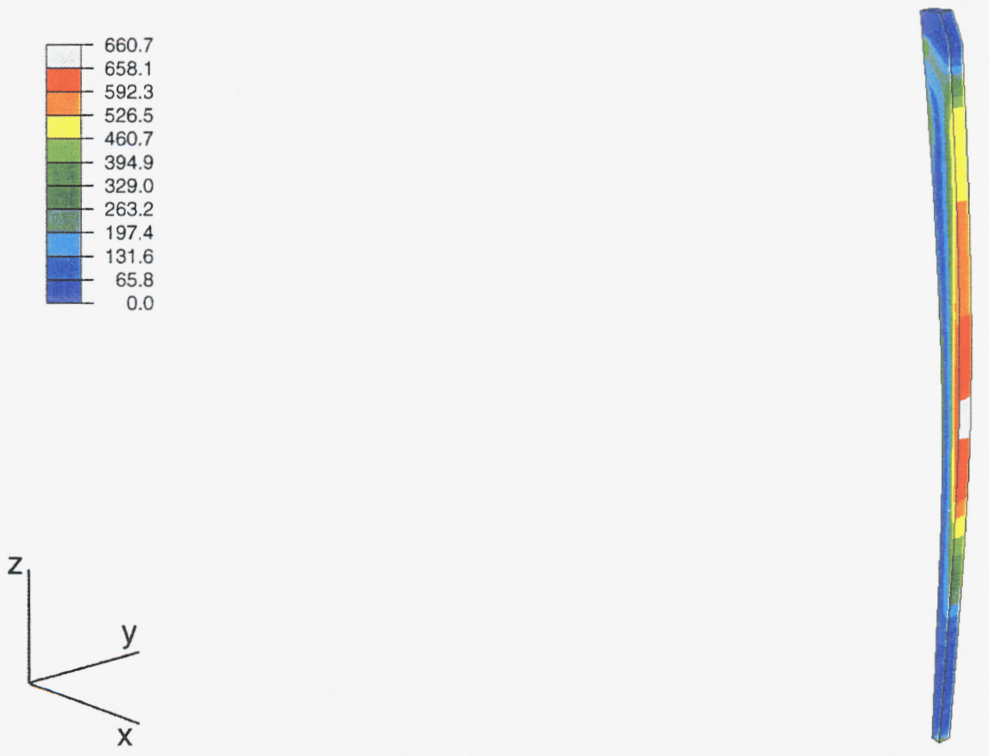

Figure 3-15. Maximum Von Mises Stress (MPa) Level Incurred by the Drip Shield Support Beam due to a 2.0-tonne (4,409-lb) Rock Block Impact per Drip Shield Segment Length

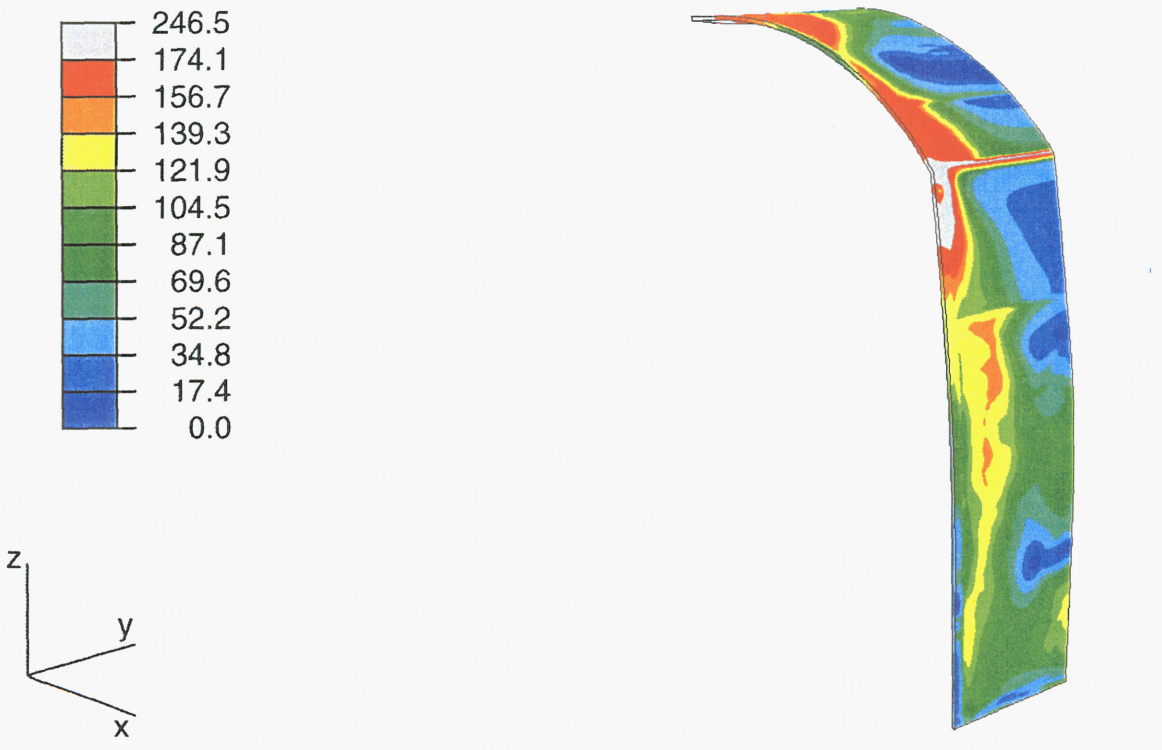

Figure 3-16. Maximum Von Mises Stress (MPa) Level Incurred by the 2-cm (0.787-in.) Thick Drip Shield Plate due to a 2.0-tonne (4,409-lb) Rock Block Impact per Drip Shield Segment Length

4 SUMMARY OF ANALYSIS RESULTS AND FUTURE PLAN

4.1 SUMMARY OF RESULTS

The results presented in this report are based on finite element analyses that employ various modeling assumptions, approximations, and simplifications. In particular, the drip shield was assumed to be at a temperature of 150 °C (302 °F), and using data obtained from the American Society of Mechanical Engineers Boiler & Pressure Vessel Code (American Society of Mechanical Engineers, 1998), a bilinear stress-strain curve was used to represent for the behavior of titanium grade 7, titanium grade 24, and Alloy 22. Moreover, to assess the potential effects of ground motion, it was assumed that the base of the drip shield was moving vertically upward at a constant rate of 1 m/s (3.28 ft/s) for the duration of the impact event.

The rock block was modeled as a linear elastic body with an infinite strength to (i) limit the energy absorbed or dissipated by the rock block to a minimum, (ii) provide a stable and consistent surface contact interface with the drip shield, and (iii) conservatively estimate the damage incurred by the drip shield and, subsequently, the waste package.

Three different drip shield-rock block impact cases were investigated. These cases included 0.5-, 1.0-, and 2.0-tonne (1,102-, 2,205-, and 4,409-lb) rock block impacts. In all cases, the rock block impact velocity was assumed to be 7 m/s (22.97 ft/s). To simulate the occurrence of seismic ground motion, the invert floor was kept at a constant upward velocity of 1 m/s (3.28 ft/s) throughout the duration of the analyses.

Drip shield deflections obtained from the analyses indicate that relatively small rock block impact loads are sufficient to cause the current drip shield design to be driven into the larger waste packages. The loads transmitted to the waste package may be enough to cause localized residual stresses at the drip shield–waste package impact point and between the waste package–pallet support that can support stress corrosion cracking. Quantification of the loads transmitted to the waste package by a drip shield driven by a sufficiently large rock block has yet to be completed.

Plastic deformation was experienced by the 2-cm (0.787-in.) thick titanium grade 7 plates for all three cases. Rock block loads of 1.0-tonne (2,205 lb) per drip shield segment length or greater were observed to cause localized bulkhead Von Mises stresses that exceed the yield stress of titanium grade 24. Von Mises stresses in the support beam greater than the titanium grade 24 yield stress were observed in the 2.0-tonne (4,409-lb) per drip shield segment length only.

4.2 FUTURE PLAN

The magnitude of the stresses experienced by the drip shield components during a rock block impact are affected by the ground motion transmitted through the invert floor. As a consequence, potential resonance of the individual engineered barrier subsystem component structures generated by the seismic ground motion and development of concomitant dynamic load amplification factors should be an area of continued study. These effects are strongly dependent on the design details of the engineered barrier subsystem component structures and the time–history characterization that will define the seismic ground motion for the proposed Yucca Mountain repository horizon.

The rockfall study will be expanded to encompass a larger range of rock block sizes and rock block fall heights so the maximum deflections and stresses can be appropriately abstracted for the Total-system Performance Assessment code. For example, to ascertain the impact loads that will breach the drip shield, rock block sizes of 4.0- and 8.0-tonnes (8,820- and 17,640-lb) per drip shield segment length are scheduled to be evaluated. Different impact velocities for all rock block sizes are also scheduled to be performed so the effects of different fall heights can be accounted in the Total-system Performance Assessment code abstractions. These abstractions will be used to determine whether the drip shield has (i) been driven into the waste package, (ii) experienced stresses sufficient to cause stress corrosion cracking, or (iii) been breached, creating water infiltration pathways that can affect waste package corrosion rates and radionuclide transport.

Modeling efforts will continue to evolve by incorporating more design details of the drip shield as they are provided by the DOE. Moreover, long-term corrosion-related degradation, initial manufacturing defects, material embrittlement, and direct seismic shaking of the drip shields will be accounted in the finite element models when the technical basis for characterization becomes available. The ultimate intent of this work is to enable an acceptable assessment of rockfall on the intended functions of the drip shield. This effort aims to produce a more realistic failure model abstraction for the SEISMO module of the Total-system Performance Assessment code and provide additional information that can be used, in part, for the resolution of the Container Life and Source Term Key Technical Issue.

5 REFERENCES

American Society for Metals International. "Material Properties Handbook: Titanium Alloys." Materials Park, Ohio: American Society for Metals International. 1994.

American Society for Testing and Materials. "Standard Specification for Titanium and Titanium Alloy Strip, Sheet, and Plate." Philadelphia, Pennsylvania: American Society for Testing and Materials. pp. B265–98. 1998.

American Society of Mechanical Engineers. "American Society of Mechanical Engineers Boiler and Pressure Vessel Code." New York City, New York: American Society of Mechnical Engineers. 1995.

American Society of Mechanical Engineers. "American Society of Mechanical Engineers Boiler and Pressure Vessel Code." New York City, New York: American Society of Mechanical Engineers. 1998.

CNWRA. "Technical Assessment of Structural Deformation and Seismicity at Yucca Mountain, Nevada." San Antonio, Texas: CNWRA. 2001.

CRWMS M&O. "Probabilistic Seismic Hazard Analyses for Fault Displacement and Vibratory Ground Motion at Yucca Mountain, Nevada." WBS 1.2.3.2.8.3.6. Oakland, California: DOE. 1998a.

———. Chapter 10: Disruptive Events. "Total System Performance Assessment—Viability Assessment (TSPA-VA) Analyses Technical Basis Document." B00000000–01717–4301–00010. Revision 00A. Las Vegas, Nevada: TRW Environmental Safety Systems, Inc. 1998b.

———. "License Application Design Selection Report." B00000000–01717–4600–00123. Revision 01. Las Vegas, Nevada: CRWMS M&O. 1999a.

———. "Enhanced Design Alternative II Report." B00000000–01717–5705–00131. Revision 00. Las Vegas, Nevada: CRWMS M&O. 1999b.

———. "Drip Shields LA Reference Design Feature Evaluation #2." B00000000–01717–2200–00207. Revision 00. Las Vegas, Nevada: CRWMS M&O. 1999c.

———. "Drift Degradation Analysis." ANL–EBS–MD–000027. Revision 00. Las Vegas, Nevada: CRWMS M&O. 1999d.

———. "Drift Degradation Analysis." ANL–EBS–MD–000027. Revision 01. Las Vegas, Nevada: CRWMS M&O. 2000a.

———. "Design Analysis for the Ex-Container Components." ANL–XCS–ME–000001. Revision 00. Las Vegas, Nevada: CRWMS M&O. 2000b.

———. "Rockfall on Drip Shield." CAL–EDS–ME–000001. Revision 00. Las Vegas, Nevada: CRWMS M&O. 2000c.

———. "Yucca Mountain Science and Engineering Report." DOE/RW–0539. Las Vegas, Nevada: CRWMS M&O. 2001.

DOE. "Viability Assessment of a Repository at Yucca Mountain, Overview." DOE/RW–0508. Las Vegas, Nevada: DOE. Office of Civilian Radioactive Waste Management. 1998a.

———. "Viability Assessment of a Repository at Yucca Mountain." Volume 2: Preliminary Design Concept for the Repository and Waste Package. DOE/RW–0508V2. Las Vegas, Nevada: DOE. Office of Civilian Radioactive Waste Management. 1998b.

Ghosh, A., J. Stamatakos, S. Hsiung, R. Chen, A.H. Chowdhury, and H.L. McKague. "Key Technical Issue Sensitivity Analysis with SEISMO and FAULTO Modules Within the Total-system Performance Assessment (Version 3.1.1) Code." San Antonio, Texas: CNWRA. 1998.

Gute, G.D., T. Krauthammer, S.M. Hsiung, and A.H. Chowdhury. "Assessment of Mechnical Response of Waste Packages Under Repository Environment—Progress Report." San Antonio, Texas: CNWRA. 1999.

Gute, G.D., A. Ghosh, S.M. Hsiung, and A.H. Chowdhury. "Assessment of Mechnical Response of Drip Shields Under Repository Environment—Progress Report." San Antonio, Texas: CNWRA. 2000.

Hibbitt, Karlsson & Sorensen, Inc. ABAQUS/Explicit User's Manual, Version 5.8. Pawtucket, Rhode Island: Hibbitt, Karlsson & Sorensen, Inc. 1998.

Hill, B.E. and J.S. Trapp. "Sensitivity Analysis for Key Parameters in the VOLCANO and ASHPLUME Modules of the Total-system Performance Assessment Version 3.1 Code." San Antonio, Texas: CNWRA. 1997.

Hill, B.E. and C.B. Connor. "Technical Basis for Resolution of the Igneous Activity Key Technical Issue." San Antonio, Texas: CNWRA. 2000.

Hsiung, S.M., G-H. Shi, and A.H. Chowdhury. "Assessment of Seismically Induced Rockfall in the Emplacement Drifts of the Proposed Repository at Yucca Mountain—Progress Report." San Antonio, Texas: CNWRA. 2000.

Hsiung, S.M., G-H. Shi, and A.H. Chowdhury. "Assessment of Seismically Induced Rockfall in the Emplacement Drifts of the Proposed Repository at Yucca Mountain, Nevada." San Antonio, Texas: CNWRA. 2001.

Mohanty, S., T.J. McCartin, and D.W. Esh. "Total-system Performance Assessment Version 4.0 Code: Module Descriptions and User's Guide." San Antonio, Texas: CNWRA. 2000.

NRC. "Input to Structural Deformation and Seismicity Issue Resolution Status Report." Revision 2. Washington, DC: NRC. 2000a.

———. " Input to Igneous Activity Issue Resolution Status Report." Revision 2. Washington, DC: NRC. 2000b.

———. "Input to Repository Design and Thermal-Mechanical Effects Issue Resolution Status Report." Revision 3. Washington, DC: NRC. 2000c.

U.S. Department of Defense. "Military Handbook: Metallic Materials and Elements for Aerospace Vehicle Structures." MIL–DBK–SH. Washington, DC: U.S. Department of Defense. 1998.